Australian Optical Society

NEWS

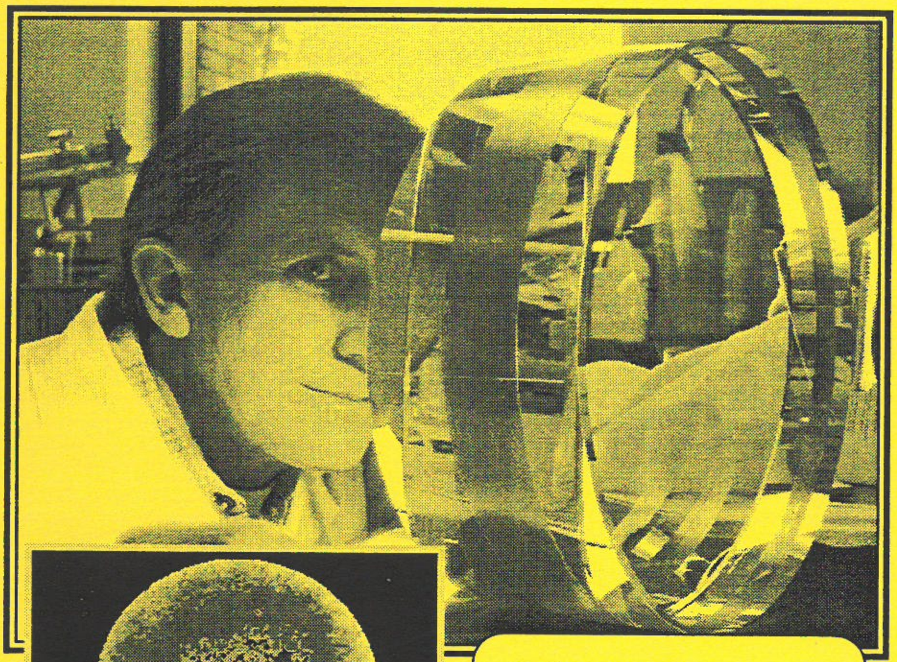
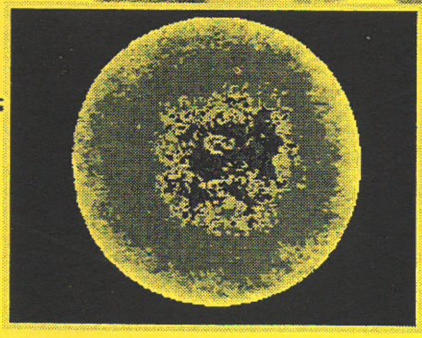

Optics for LIGO

Squeezed light spectroscopy

High power UV lasers

Waveguide characterisation

Volume 11 Issue 3

September 1997

Registered by Australia Post
Publication No: 233066 / 00021

COVER:
An example of an optical component being produced by CSIRO for the LIGO project*. The components are made from the highest quality fused silica from Corning in the US and Heraeus in Germany. The blanks alone have an average value of around $40,000 each (see the article on p19).

The purpose of the LIGO project is to detect and measure gravitational waves through their interaction with 'test' masses which double as mirrors at the ends of a long path (≈ 4 km) interferometer.

**LIGO is managed by the California Institute of Technology and Massachusets Institute of Technology.*

SUBMISSION OF COPY:
Contributions on any topic of interest to the Australian optics community are solicited, and should be sent to the editor, or a member of the editorial board. Use of electronic mail is encouraged, or else submission of hard copy together with an ASCII text file on floppy disk.

Where possible, diagrams should be contained within the document or sent as separate encapsulated post-script files. Figures on A4 paper will also be accepted.

EDITOR
Duncan Butler
CSIRO Tel. & Ind. Phys.
PO Box 218
Lindfield NSW 2070
Tel: (02) 9413 7302
Fax: (02) 9413 7474
Duncan.Butler@tip.csiro.au

DEADLINE FOR NEXT ISSUE : 7th November, 1997

SEPTEMBER 1997 **VOLUME 11 NUMBER 3**

AOS NEWS

ARTICLES

DEPARTMENTS

AOS News is the official news magazine of the Australian Optical Society. The views expressed in AOS News do not necessarily represent the policies of the Australian Optical Society.

CORPORATE MEMBERS

Australian Holographics
AVIMO Electro-Optics
British Aerospace Australia
Coherent Scientific
Electro-Optics
Francis Lord Optics
Hadland Photonics
Kidger Optics
Laser Electronics(Operations)
Lastek
Optiscan
Photon Engineering
Raymax Applications
Rofin Australia
Spectra-Physics
Warsash Scientific

AFFILIATES

OSA
(The Optical Society of America)
SPIE
(The International Society for Optical Engineering)

President's Report

by Brian Orr

I am startled to realise how rapidly 1997 is passing by, with the September issue of *AOS News* now in preparation. The seeming contraction of time is probably a function of the multitude of tasks that continually seem to crop up and require attention without delay. I doubt that I am alone in this experience, given the increased pressures that are being applied to most of us in the workplace, whether it be a university, a government institution, or a commercial setting. Mind you, I confess that I take a morbid pleasure in working under pressure. It tends to bring out the best and ensure that one devotes one's attention to things that really need to be done. "Give a job to a busy person," they say!

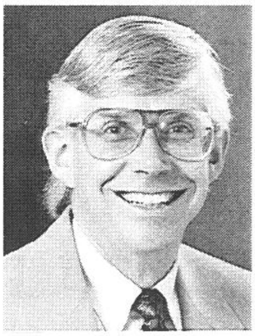

Nevertheless, it would be nice occasionally to have time to sit back and sort out one's priorities and ensure that "what really needs to be done" is actually the most important thing in absolute terms and not merely the most pressing chore. In a flashback to my schooldays, I recall a poem (entitled "Leisure" by W. H. Davies) that begins: "What is this life if, full of care, we have no time to stand and stare?". To me, that is an important question for my workplace activities as well as for my leisure time, as it should be to any practising scientist or person with an innovative mission. Sufficient opportunity to "stand and stare" (that is, in the workplace, to contemplate fresh directions, to read professional literature outside one's immediate range of interest, to communicate meaningfully with colleagues, to enjoy another person's elegant piece of research, etc.) seems hard to come by ...

I got onto this contemplative track because I intended to sit down to write a President's Report that would encourage you to take stock of your involvement in the Australian Optical Society. I had better get on with that intention, hadn't I?

We are approaching that time of year when you will need to consider renewing your subscription for AOS membership, so it is worthwhile reminding you of the various benefits that come from that source. I made a tally of these benefits a few days ago when I prepared a letter that all Australian and New Zealand members of the Optical Society of America (OSA) will receive in due course, concerning discounted joint membership arrangements for 1998. This is the outcome of a renewed agreement between AOS and OSA that was signed earlier this year and it means that you can join or renew your membership in both Societies for about AU$10 more than what it costs to belong to OSA alone. Another example of joint membership benefits is provided by the AOS's recently concluded agreement with SPIE, that provides a similar (but slightly more complicated) discount for joint AOS/SPIE membership.

In my opinion, the most outstanding feature of AOS activities is our biennial "stand-alone" conference, next to be held as AOS XI in Adelaide on 10 - 12 December 1997. This provides AOS members with a good opportunity to communicate widely with their colleagues from the local optics scene. You will find further information about this conference and its preceding specialist workshops elsewhere in this issue and on the Web at *http://www.physics.adelaide.edu.au/~mwh/aosmeet/aosmeet.html*
What you won't necessarily find there is the clear message that the ultimate success of this conference will not only depend on the excellent line-up of invited speakers and on all the careful preparations being made by the organising committee (headed by Jesper Munch), but also on whether AOS members such as yourself support it by attending and contributing your best and latest work on optical science and technology. By the time you receive this issue of *AOS News*, the October 1 deadline for submission of papers will not be far off - so the decision is yours ...

There are other important things on the AOS agenda, such as: the next joint conference in the Australian Conference on Optics, Lasers and Spectroscopy (ACOLS) series in 1998, to be held off-shore in New Zealand; the prospect of colocating our 1999 AOS XII meeting with a meeting in the Optical Guided Waves and Applications series; ongoing liaison with various international scientific conferences, such as CLEO, IQEC, and CLEO Pacific Rim; regular involvement in the activities of FASTS (the Australian science lobby organisation in Canberra); efforts over the next few months to promote the preservation of Optics as a Priority Area of the Australian Research Council.

You can maintain regular touch with many of the AOS's activities by way of our Web site, at *http://www.dap.csiro.au/OPTECH/Optics-Radiometry/aosinfo.htm*. But please don't overlook the medium of AOS communication that is in your hands as you read this message: *AOS News* itself.

Our quarterly periodical is much more than just a set of optics-related announcements and advertisements inside a canary-yellow cover. If you have not done so already, I suggest that you take some time to read the scientific/technical articles that are contained in this issue of *AOS News - especially* if they don't fall within your own area of specialisation.

My point is that we should take some "time to stand and stare" (as the poem says) at what our other AOS colleagues are doing, through their carefully prepared accounts of the aspects of optics that particularly interest them. Let's not be so preoccupied with things that we think really need to be done that we miss opportunities to learn from others' expertise and enthusiasm.

With that in mind, I look forward to seeing you at AOS XI in Adelaide this coming December.

-Brain Orr

AOS XI

The Eleventh Conference of the Australian Optical Society

The University of Adelaide, 10-12 December 1997.

Final Call for Papers (Deadline : October 1)

Contributions are now invited in any area of optics

- There will be a number of invited talks (30 min) as well as contributed talks (15min) and poster sessions.
- The majority of presentations will be posters.
- Contributed papers to the AOS conference, and the associated workshops, can be submitted for publication in a special issue of *Optical and Quantum Electronics*.
- A trade exhibit is planned.

INVITED PLENARY SPEAKERS

Confirmed invited speakers are listed below within broad subject areas. The sessions are tentatively organised around these areas.

GENERAL OPTICS

Professor **Duncan Moore**, University of Rochester
"Gradient Index Optics (natural and manmade)"
Professor **Michael. Roggemann**, Wright-Patterson/Michigan Technological University
"Improvement of ground-based telescope resolution using micro-electro-mechanical deformable mirrors"

LASERS AND PHOTONICS

Professor **Wilson Sibbet**, St Andrews University
title to be announced
Professor **Jim Piper**, Macquarie University. The 1997 AOS Medal Lecture:
"Engineering gain — developments in high-power, high-beam-quality copper lasers"

SPECTROSCOPY AND ATOM OPTICS

Dr **Neil Manson**, ANU
"Concepts of NMR in nonlinear and quantum optics"
Dr **Peter Hannaford**, CSIRO
"Magnetostatic Optics for Ultracold Atoms"

FOURIER OPTICS AND HOLOGRAPHY

Professor **Henri Arsenault**, Universite Laval
"Invariant pattern recognition: scale and out-of-plane rotations"

INTERFEROMETRY

Professor **Barry Barish**, Caltech/Principal Investigator of LIGO
title to be announced

MEDICAL OPTICS

Professor **Ian Hodgkinson**, Otago University
"Photoscreening the young and the elderly — detecting refractive errors and mapping cataracts"
Professor **Doug Coster**, Flinders University
"Optics and lasers in the preservation of vision"

NONLINEAR OPTICS AND APPLICATIONS

Professor **Barry Luther-Davies**, Australian National University
"Optical Spatial Solitons in Saturating Nonlinear Media"

ASSOCIATED WORKSHOPS

Three workshops associated with the conference are planned:

Quantum Coherence and Information Processing
homepage http://www.physics.adelaide.edu.au/~mwh/qip/qiproc.html
Propagation and Imaging Science
homepage http://www.physics.adelaide.edu.au/~mwh/prop/ws-hom~1.htm
Thermal Noise Limitations in Gravitational Wave Interferometry
homepage http://www.physics.adelaide.edu.au/optics/thermal.html

PUBLIC LECTURE

A public lecture associated with the AOS conference and the Quantum Coherence and Information Processing workshop is also planned: the speaker will be Dr Dave Wineland, NIST, on "Quantum computation".

CONFERENCE PROCEEDINGS

A special issue of the journal *Optical and Quantum Electronics* is scheduled to appear in 1998, devoted to this conference. All submissions will be refereed and should conform to the journal format. If you intend to make use of this opportunity, you should prepare the typed manuscript in advance and hand in four copies (including the original) at either the AOS conference registration desk or the workshop registration desk. The requirements of the journal for the preparation of typescripts are given in these instructions to authors
(see http://www.physics.adelaide.edu.au/~mwh/prop/autho.htm)

ACCOMMODATION

Low cost accommodation has been reserved at the residential wing of the Royal Adelaide Hospital, next to the University of Adelaide campus on North Tce. A wide variety of hotels is available close to the University for those participants who opt to make their own arrangements. Further information is to be found on the accommodation booking form via the conference homepage.

CONFERENCE FEES

AOS Member $190 , Non-member $220 , Students $90

The fee for non-members includes membership of the AOS for one year. There will be a limited amount of travel assistance available for students.

ORGANISING COMMITTEE

J Munch (chair), M Hamilton (secretary), P Veitch (treasurer), D McCoy, University of Adelaide
P Teubner, Flinders University
N Jones, A Masters, Coherent Scientific Pty. Ltd.
J Hermann (journal liason), R Seymour, A-M Grisogono (trade exhibit), DSTO

IMPORTANT NOTE

Registration and submission of papers will be conducted as far as possible through the internet; please get the appropriate forms through the conference home-page:
http://www.physics.adelaide.edu.au/~mwh/aosmeet/aosmeet.html

For further information please contact:-
Jesper Munch, University of Adelaide, Tel: (08) 8303 4749, Fax: (08) 8232 6541
Email: jmunch@physics.adelaide.edu.au

AUSTRALIAN OPTICAL SOCIETY

POSTGRADUATE STUDENT PRIZE

A. Preamble

The Australian Optical Society wishes to encourage participation in national and international conferences by high-quality postgraduate students. To this end, the Society has instituted an award, the Australian Optical Society Postgraduate Student Prize. This will take the form of a grant to assist the grantee to attend a conference in optics or a related field. For 1998, the award will be valued at up to $1500. The Society now invites applications from suitably qualified people for this prize for 1998.

B. Prerequisites

An applicant must be: (1) a citizen or permanent resident of Australia, (2) a member of the Australian Optical Society, (3) enrolled in a postgraduate research degree in Australia at 31 October 1997, with a project in an optically related area. Non-members of the AOS may join the Society concurrently with their application for the prize. (Application forms are available in *AOS News*, or may be obtained from the Treasurer or Secretary). The prize cannot be awarded more than once to any individual.

C. Selection criteria

An applicant must be sufficiently advanced in the research project to have obtained significant results in optics or a related area, such that those results are suitable for presentation at a proposed conference that falls in the twelve month period commencing 1 December 1997. It is expected that the presentation at the proposed conference would take the form of a research paper, invited or contributed, oral or poster. The successful applicant will be expected to write a summary of the conference for *AOS News*.

Preference will be given in the selection procedures to applicants who intend to use the prize to attend and present their research results at a major conference outside Australia or New Zealand.

It is not essential that the results to be presented should already have been accepted for presentation at the proposed conference at the time of application, but no payment of the prize will be made until evidence of such acceptance is provided to the Society. Applicants are encouraged to provide tangible evidence of the results likely to be presented at the proposed conference (for example, in the form of an outline of a paper that has been accepted or submitted or is being prepared for that conference) and to make clear the benefits that would arise from their attendance at that conference.

The AOS award is not intended to cover the full cost of the applicant's attendance at the proposed conference. Wherever possible, applicants should identify means by which their research group and/or institution is likely to make a substantial contribution to their travel costs. Evidence of any such supplementary support should be provided (for example, by an undertaking in the supervisor's letter of recommendation). However, students with no identifiable supplementary travel support will not be disadvantaged in the selection process.

Since the research supervisor's report is a major factor in the assessment process, supervisors should be prepared to rank their students against the selection criteria if contacted by the selection committee.

D. Application Details

1. Curriculum vitae;
2. List of publications, conference papers, theses, reports, etc.;
3. Details of postgraduate research project;
4. Details of proposed conference (including its status and relevance to optics);
5. Details of participation in the conference (nature of contribution as specified above);
6. Details of predicted expenses, as well as other (probable or confirmed) sources of funding for attendance at the conference;
7. Reports from the candidate's research supervisor and one other referee;
8. Statement that the candidate is a citizen or permanent resident of Australia;
9. Statement of agreement to write a summary of the conference for *AOS News*.

Applications should be sent to the Secretary:

Dr Clyde Mitchell
CSIRO DMST
Private Bag 33
Clayton South
Victoria 3169

and **must be received by 31 October 1997**. The winner will be announced early in 1998.

OPTICS GRAPEVINE

News from the World of Optics

Editorial

Thanks to the efforts of the editorial board and the AOS membership we have a bumber issue this September. Many thanks to the board and the authors for their time and effort.

This issue of *AOS News* has been one of the more difficult to compile, partly due to the number of articles, and partly due to the appearance of a new version of Microsoft Word (Word 97). New versions always make it difficult for me to translate submitted articles. (I use Word for Windows Version 2.0c for most sections of the *AOS News* — in case anyone is interested!).

I would like to draw your attention to the information about the AOS conference on pages 4 and 5. Note that abstracts are due on the 1st of October. I am hoping to get the December issue out in the week before the conference, in which case I will try to print a more thorough preview.

Duncan Butler

All electronic publishing - Optics Express -

Optics Express is the all-electronic journal for optics published by the Optical Society of America. Optics Express publishes original, peer-reviewed articles that report new developments of interest to the optics community in all fields of optical science and technology. Drawing on unique features of the electronic medium, Optics Express provides authors the opportunity to present data and results in ways not possible in print, with the potential for greatly reduced time to publication.

Optics Express articles will be archived electronically and made available online indefinitely. In addition, individual volumes will be made available in a CD-ROM format on a regular basis. Optics Express articles are uniquely and permanently identified by page, issue, and volume number.

Optics Express may be accessed via OpticsNet at www.osa.org. The reading, searching, printing and submitting functions of Optics Express are currently most easily done with the following freely available Internet utilities:

Netscape Navigator™
Adobe Acrobat™ Plug-in
Quicktime™ Multimedia Plug-in

Some search and submission features are not currently available to users of other browsers. Microsoft Internet Explorer 3.0 is expected to be supported soon.

Of interest...

The **Casimir force** (between conducting plates as a result of the exclusion of some of the possible cavity modes) has been accurately measured. (*Phys.Rev.Lett.* **78**, p5 1997)

Researchers at MIT have developed an output coupler for atoms in a Bose-Einstein condensate. Such a condensate can be made at very low temperatures in a magnetic trap. An oscillating magnetic field allows pulses of atoms (or "Bose-condensed droplets") to escape. The device may be regarded as a primitive **atom laser**. (*Phys.Rev.Lett* **78**, p582 1997)

Atomic Spectroscopy with a Squeezed Vacuum Field

Zbigniew Ficek
Department of Physics and Centre for Laser Science,
The University of Queensland, Brisbane, Qld 4072, Australia

The interaction between atoms and squeezed light leads to many novel and unusual effects not observed in spectroscopy with conventional radiation sources. We explore those effects which have a nonclassical character and discuss their unusual properties.

1. Introduction

All forms of light exhibit inherent and unavoidable random fluctuations. For the most part these fluctuations arise from random and uncontrolled changes in the light source which lead to changes in the frequency and amplitude of the light wave. With the help of new techniques most of these influences can be removed. However, even in highly stabilised sources of light, the generated fields are still subject to fluctuations arising from the quantum nature of electromagnetic radiation. This source of noise was formerly believed to be an insuperable barrier to optical measurements.

In the last two decades theoretical studies followed by experimental measurements [1] have shown that this barrier can be circumvented, and light fields with reduced ("squeezed") fluctuations can be generated. The possibility of obtaining light fields whose fluctuations are less than those expected from the laws of quantum mechanics allows researchers to perform experiments with greater precision than possible with laser light. Moreover, promises of noise-free optical measurements and information transmission has also raised hopes for new applications. One such possibility is gravity-wave detection based on optical interferometry, and other proposals include computing, cryptography, spectroscopy and laser technology.

2. Squeezed Light

To understand squeezed light, recall that the electromagnetic field can be described by two independent components — its amplitude and phase or, alternatively, by quadrature phase components. According to quantum mechanics, these components are represented by noncommuting Hermitean operators (observables). The Heisenberg uncertainty principle predicts that it is never possible to be absolutely precise in measuring one of two noncommuting observables. The product of the variances of the two noncommuting observables must be greater than or equal to one-half of the absolute value of their commutator. Thermal sources of light emit chaotic fields, with variances greater than this commutator. Ideal lasers emit coherent light, which has quadratures whose variances are equal to the commutator. These sources exhibit only quantum noise, equal to the fluctuations of the vacuum. There are, however, fields such that the variance of one of the two noncommuting observables is smaller than the vacuum fluctuations. Such a field is referred to as squeezed light. In squeezed light the quantum fluctuations in one quadrature component are reduced below their vacuum values at the expense of increased fluctuations in the other component, such that the uncertainty relation is not violated. Squeezed light is one form of nonclassical light; it cannot be mathematically described as a superposition of coherent states with nonnegative weights.

3. Producing Squeezed Light

Squeezed light has attracted considerable interest since the possibility of generating it was first suggested by Stoler [2] and Yuen [3]. A number of experimental groups have been involved in its generation. Slusher et al [4] generated for the first time a squeezed light in which a 7% noise reduction below the vacuum level was observed. Wu et al [5] reported more than 50% reduction of noise below the vacuum limit in an optical oscillator. Heidmann et al [6] used a two-mode optical parametric oscillator operating above threshold to generate two highly correlated beams of light. The measured noise in the intensity difference of the two beams was 30% below the vacuum limit. In an improved experiment, Debuisschert et al [7] observed a 69% noise reduction in the intensity difference. Yamamoto et al [8] developed semiconductor lasers with intensity fluctuations reduced by 95% below the vacuum noise level.

Kimble and co-workers [9] have developed a frequency tunable source of a squeezed vacuum field with about 70% noise reduction below the vacuum level. In their experiment, a squeezed field is generated via nondegenerate parametric down conversion. In this nonlinear process two modes, called the signal and idler modes, are generated at frequencies ω_1 and ω_2 such that $\omega_1 + \omega_2 = 2\omega_o$, where $2\omega_o$ is the frequency of the pump field. The squeezed vacuum generated in this nonlinear process does, of course, contain photons — the word "vacuum" means that the average amplitude of the squeezed field is equal to zero.

4. Nonclassical Spectroscopy with Two-Level Atoms

The successful generation of squeezed light has encouraged theoretical research into its applications. An obvious possibility is the field of atomic spectroscopy, since the radiative properties of atoms are intimately related to fluctuations in the electromagnetic field. The idea of squeezed light atomic spectroscopy was originally due to Gardiner [10], who showed that squeezed light can indeed alter the fundamental radiative properties of atoms. He predicted that, in a broadband squeezed vacuum, the two polarisation components of the atom are damped at different rates, one reduced and the other enhanced compared to that in the normal vacuum.

Following Gardiner's analysis, define the atomic polarisation quadratures S_X and S_Y by

$$S^{\pm} = \frac{1}{2}(S_X \pm iS_Y), \qquad (1)$$

where $S^{+}\left(S^{-}\right)$ is the atomic raising (lowering) dipole moment operator. The equations of motion for the average quadrature operators can be derived in the form [10]

$$\begin{aligned} <\dot{S}_X> &= -\Gamma\left(\frac{1}{2} + N + |M|\right) < S_X >, \\ <\dot{S}_Y> &= -\Gamma\left(\frac{1}{2} + N - |M|\right) < S_Y >, \end{aligned} \qquad (2)$$

where Γ is the spontaneous emission rate in the normal vacuum and N, $|M|$ are the squeezing parameters. It can seen that the two polarisation quadratures are damped at different rates provided that $|M| \neq 0$.

In fact, these rates are proportional, respectively, to the variances of the maximally unsqueezed and maximally squeezed quadrature phases of the input squeezed vacuum field. In order to show this, we consider correlation functions for the squeezed vacuum field operators. The mode annihilation and creation operators of a broadband squeezed vacuum field satisfy the following correlation functions, characteristic of the output of degenerate or non-degenerate parametric oscillators [11]

$$\begin{aligned} &\langle a(\omega_i)\rangle = \langle a^{\dagger}(\omega_i)\rangle = 0, \\ &\langle a(\omega_i)a^{\dagger}(\omega_j)\rangle = [N(\omega_i)+1]\delta(\omega_i - \omega_j), \\ &\langle a^{\dagger}(\omega_i)a(\omega_j)\rangle = N(\omega_i)\delta(\omega_i - \omega_j), \\ &\langle a(\omega_i)a(\omega_j)\rangle = M(\omega_i)\delta(2\omega_S - \omega_i - \omega_j), \end{aligned} \qquad (3)$$

where ω_S is the carrier frequency of the squeezed field, $N(\omega_i)$ is the squeezing intensity (which is proportional to the number of photons in the squeezed field), and $M(\omega_i) = |M(\omega_i)|\exp(i\phi_S)$ characterises the correlations between two modes of frequencies ω_i and $2\omega_S - \omega_i$, and ϕ_S is the phase of the squeezed field. When the squeezing intensity is symmetric (relative to ω_s), the correlations between the modes obey the inequality

$$|M(\omega_i)| \leq \sqrt{N(\omega_i)[N(2\omega_S - \omega_i)+1]}. \qquad (4)$$

Introducing the quadrature operators

$$\begin{aligned} X_1 &= \frac{1}{2}(a^{\dagger} + a), \\ X_2 &= \frac{1}{2i}(a^{\dagger} - a), \end{aligned} \qquad (5)$$

which satisfy the commutational relation

$$[X_1, X_2] = \frac{1}{2i}, \qquad (6)$$

we find from Eqs. (3) and (5), that the variances of the quadrature operators of the squeezed vacuum field are given by

$$\begin{aligned} \Delta X_1^2 &= \frac{1}{2}\left(\frac{1}{2} + N + |M|\right), \\ \Delta X_2^2 &= \frac{1}{2}\left(\frac{1}{2} + N - |M|\right), \end{aligned} \qquad (7)$$

where $N = N(\omega_S)$ and $|M| = |M(\omega_S)|$ are the maximal values of the squeezing parameters calculated at the carrier frequency ω_S.

The effect of the squeezing correlations $|M|$ is to reduce the fluctuations in the quadrature component X_2 at the expense of the increased fluctuations in the conjugate quadrature component X_1. This unequal distribution of the fluctuations between the two quadratures leads to the unequal damping rates of the quadrature atomic operators seen in Eq. (2). For $|M| = \sqrt{N(N+1)}$ the damping rate of the S_Y component can be reduced below the normal vacuum level, $\Gamma/2$, and approaches zero for very large intensities $(N >> 1)$ of the squeezed vacuum field.

It should be noted here, that the reduction of the damping rate below the normal vacuum level results from the presence of the additive factor of +1 under the square root in Eq. (4). This factor arises from the quantum nature of the squeezed field — from the fact that the field operators $a(\omega_i)$ and $a^{\dagger}(\omega_i)$ do not commute. Therefore, the + 1 can be said to manifest the nonclassical character of the squeezed vacuum field. For a classical field, where the operators $a(\omega_i)$ and $a^{\dagger}(\omega_i)$ are treated as numbers, the field correlations can have the maximum value $|M(\omega_i)| = N(\omega_i)$. Thus, mode correlations with $0 < |M| \leq N$ may be generated by a classical field, whereas correlations with $N < |M| \leq \sqrt{N(N+1)}$ can only be described quantum mechanically. These extra correlations over the maximum classical value $|M| = N$ can produce dramatic effects which can be regarded as nonclassical.

5. Nonclassical Spectroscopy with Three-Level Atoms.

The effort to demonstrate the reduction of the decay rate below the normal vacuum level has stimulated researchers to examine other optical systems interacting with a squeezed vacuum field. Many interesting modifications of radiative properties of atoms in the presence of a squeezed vacuum field have been predicted [12]. Examples include subnatural linewidths and dispersive profiles in fluorescence and absorption spectra [13-21], squeezing-induced transparency [22], population trapping [23], amplification without population inversion [24], a violation of the Boltzmann distribution of the populations of the atomic states [25,26], two-photon population inversions [25-27], and linear rather than quadratic dependence on the intensity of the two-photon transition rate [25,28,29].

Although the presence of a squeezed vacuum field is essential in the generation of all these novel effects, only a few of them can be regarded as nonclassical in the sense that they are produced by the excess of the two-mode correlations $|M|$ between a squeezed vacuum and a maximally correlated classical field. One effect which *can* be regarded as nonclassical is subnatural linewidths in fluorescence and absorption spectra, which arise from the reduction of the spontaneous emission damping rates below the vacuum level. Other examples include the effects resulting from the process of a two-photon absorption between atomic levels. Such a situation can appear in the interaction of a three-level cascade system with a squeezed vacuum field.

Consider a three-level atom in the cascade configuration (Figure 1) interacting with a squeezed vacuum field of carrier frequency ω_S. For simplicity, we assume that the squeezed field is in a two-photon resonance with the atom, ie. $2\omega_S = \omega_1 + \omega_2$, where ω_1 and ω_2 are the transition frequencies between the atomic levels $|2\rangle \to |1\rangle$ and $|3\rangle \to |2\rangle$, respectively. The spontaneous transition rates between the atomic levels are γ_2 and γ_1, respectively, for the $|3\rangle \to |2\rangle$ and $|2\rangle \to |1\rangle$ transition.

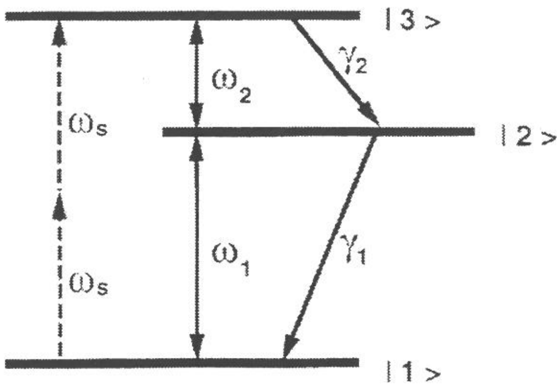

***Figure 1**: Schematic diagram of a three-level atom in the cascade configuration driven by a squeezed vacuum field of the carrier frequency ω_S.*

The steady-state populations of the states $|2\rangle$ and $|3\rangle$ are [25]

$$\rho_{22} = \frac{\eta N(\eta N+1) - \eta^2 |M|^2}{3\eta^2 N^2 + 3\eta N + 1 - 3\eta^2 |M|^2}, \tag{8}$$

$$\rho_{33} = \frac{\eta^2 N^2 W - \eta^2 |M|^2 (W - 1 - \alpha)}{W\left(3\eta^2 N^2 + 3\eta N + 1 - 3\eta^2 |M|^2\right)}, \tag{9}$$

where $\alpha = \gamma_2/\gamma_1$ and $W = \alpha + \eta N(1+\alpha)$. The parameter η describes the matching of the incident squeezed vacuum modes to all the modes coupled to the atom. For perfect matching η = 1, whereas η < 1 for imperfect matching. For a classical field with $|M| = N$ the populations reduce to:

$$\rho_{22} = \frac{\eta N}{3\eta N + 1}, \tag{10}$$

$$\rho_{33} = \frac{\eta^2 N^2 (1+\alpha)}{W(3\eta N + 1)}. \tag{11}$$

For low intensities (N << 1) the population in the state $|3\rangle$ is proportional to N^2, showing that in classical fields the population exhibits a quadratic dependence on the intensity of the driving field. Moreover, the ratio

$$\frac{\rho_{33}}{\rho_{22}} = \frac{\eta N(1+\alpha)}{\alpha + \eta N(1+\alpha)} < 1, \tag{12}$$

indicates that the populations obey a Boltzmann distribution with $\rho_{11} > \rho_{22} > \rho_{33}$. However, with a minimum uncertainty squeezed vacuum field, for which $|M|^2 = N(N+1)$, the populations are given by

$$\rho_{22} = \frac{\eta N(1-\eta)}{3\eta(1-\eta)N+1}, \qquad (13)$$

$$\rho_{33} = \frac{\eta^2 N + \eta^2 N^2 (1-\eta)(1+\alpha)}{(\alpha + \alpha\eta N + \eta N)[3\eta(1-\eta)N+1]}. \qquad (14)$$

The population in the excited state $|3\rangle$ exhibits both linear and quadratic dependence on the intensity of the squeezed vacuum field. For low intensities (N << 1) or perfect matching $(\eta \approx 1)$ the linear term dominates, which is the direct modification of the two-photon absorption $|1\rangle \rightarrow |3\rangle$. In a squeezed vacuum field the two-photon correlations enable the transition $|1\rangle \rightarrow |3\rangle$ to occur in a "single step" proportional to N. The ratio between the stationery populations is now given by

$$\frac{\rho_{33}}{\rho_{22}} = \frac{\eta + \eta N(1+\alpha)(1-\eta)}{\alpha(1-\eta) + \eta N(1+\alpha)(1-\eta)}, \qquad (15)$$

which can be larger than 1. This happens for $\eta > \alpha/(1+\alpha)$, indicating that for a good matching of the squeezed modes to all the modes coupled to the atom, the level populations no longer obey a Boltzmann distribution. Furthermore, for $\eta \approx 1$ and $\alpha << 1$ the population in the state $|3\rangle$ approaches one $(\rho_{33} \approx 1)$, indicating that a nearly-complete population inversion is possible in a three-level cascade atom driven by a squeezed vacuum field.

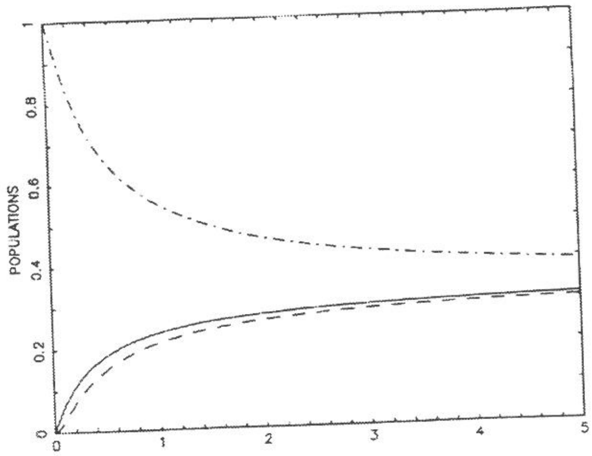

Figure 2: Populations of the atomic states as a function of the squeezing intensity N for a classical squeezed field with $|M| = N, \eta = 0.8$, *and* $\alpha = 0.1$: ρ_{22} *(solid line),* ρ_{33} *(dashed line),* ρ_{11} *(dashed-dotted line).*

Figure 2 shows the populations of the atomic states as a function of N for a classical squeezed field with $|M| = N$, $\eta = 0.8$ and $\alpha = 0.1$. There is no population inversion between the atomic states, and for small N the population ρ_{33} exhibits a quadratic dependence on the intensity N. In Figure 3, we show the populations as a function of N for a squeezed vacuum field with nonclassical correlations, $|M| = \sqrt{N(N+1)}$. In this case there are inversions between the atomic states. Moreover, for small N the population ρ_{33} exhibits a linear dependence on the intensity N. The novel features seen in Figure 3 arise from the presence of the factor +1 in Eq. (4), indicating their nonclassical character.

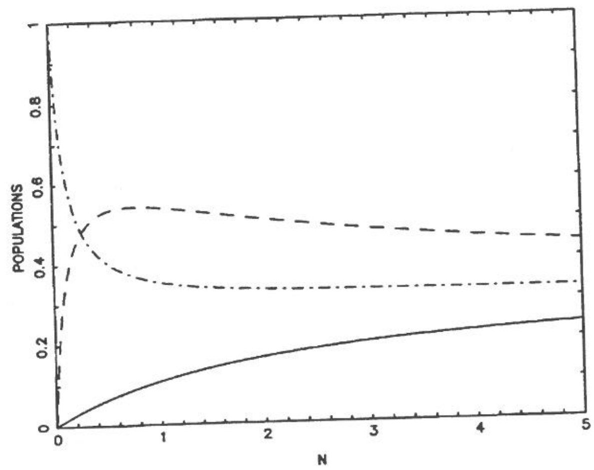

Figure 3: Populations of the atomic states as a function of the squeezing intensity N for a squeezed field with nonclassical correlations $|M| = \sqrt{N(N+1)}, \eta = 0.8$ *and* $\alpha = 0.1$: ρ_{22} *(solid line),* ρ_{33} *(dashed line),* ρ_{11} *(dashed-dotted line).*

The challenge to demonstrate nonclassical effects in the interaction between atoms and a squeezed field is not only on theoretical grounds. Recently, Kimble and co-workers [30] at the California Institute of Technology have observed experimentally the linear dependence of the population, ρ_{33}, on the squeezing intensity, N. In their experiment, the squeezed vacuum field was generated by an optical parametric oscillator (OPO) operating below threshold. The output of the OPO consists of two low intensity, but strongly correlated, beams of frequencies ω_1 and ω_2, symmetrically located about the carrier frequency $\omega_s = (\omega_1 + \omega_2)/2$. The correlation exhibits nonclassical behaviour, as expressed by Eq. (4).

This squeezed field was then focussed into a magneto-optic trap containing atomic cesium. The cesium atoms behave as three-level cascade atoms with transition wavelengths λ_{32} = 917 nm and λ_{21} = 852 nm. The output beams of the OPO were tuned to these atomic transitions. By monitoring of the intensity of the 917 nm fluorescence (which is proportional to the population ρ_{33}) the experimental team observed that for small intensities of the input beams the population ρ_{33} exhibits a linear dependence on intensity. The observed departure from the quadratic intensity dependence observed with a classical field gives compelling evidence for the nonclassical character of the squeezed vacuum field.

Most recently, Kimble's group has performed another experiment [31], based on the theory developed in Reference [25], in which they have measured a phase-sensitive modulation of the population ρ_{33} due to squeezing correlations. These two pioneering experiments demonstrate that non-classical atomic spectroscopy offers new physical effects not obtained with conventional radiation sources.

6. Summary.

We have explored the role sources of squeezed light in atomic spectroscopy. Many interesting modifications of radiative properties of atoms in the presence of squeezed light have been predicted. We have particularly explored those effects which have a nonclassical character. All of the effects are new to the field of atomic spectroscopy and cannot be observed with classical excitation fields.

Acknowledgments

I would like to thank my colleagues Peter Drummond, Bryan Dalton, Stuart Swain and Ridza Wahiddin for their many contributions to this research.

References

[1] For references see the special issues of Journal Mod. Opt. **34** (6/7) (1987) and J. Opt. Soc. Am. **B4**, (10) (1987).

[2] D. Stoler, Phys. Rev. Lett. **33**, 1397 (1974).

[3] H.P. Yuen, Phys. Rev. **A13**, 2226 (1976).

[4] R.M. Slusher, L.W. Hollberg, B. Yurke, J.C. Mertz and J.F. Valley, Phys. Rev. Lett. **55**, 2409 (1985).

[5] L.A. Wu, H.J. Kimble, J.L. Hall and H. Wu, Phys. Rev. Lett. **57**, 2520 (1986).

[6] A. Heidmann, R. Horowicz, S. Reynaud, E. Giacobino, C. Fabre and G. Camy, Phys. Rev. Lett. **59**, 2555 (1987).

[7] T. Debuisschert, S. Reynaud, A. Heidmann, E. Giacobino and C. Fabre, Quantum Opt. **1**, 3 (1989).

[8] Y. Yamamoto, M. Imoto and S. Machida, Phys. Rev. **A32**, 2287 (1986).

[9] L.A. Wu, M. Xiao and H.J. Kimble, J. Opt. Soc. Am. **B4**, 1465 (1987).

[10] C.W. Gardiner, Phys. Rev. Lett. **56**, 1917 (1986).

[11] M.J. Collett and C.W. Gardiner, Phys. Rev. **A30**, 1386 (1984).

[12] For a review see A.S. Parkins, in *Modern Nonlinear Optics*, part II, eds. M. Evans and S. Kielich (Wiley, New York, 1993) p.607.

[13] H.J. Carmichael, A.S. Lane and D.F. Walls, J. Mod. Opt. **34**, 821 (1987).

[14] H. Ritsch and P. Zoller, Phys. Rev. **A38**, 4657 (1988).

[15] A.S. Parkins, Phys. Rev. **A42**, 6873 (1990).

[16] G. Yeoman and S.M. Barnett, J. Mod. Opt. **43**, 2037 (1996).

[17] M.R. Ferguson, Z. Ficek and B.J. Dalton, Phys. Rev. **A54**, 2379 (1996).

[18] Z. Ficek, B.J. Dalton and M.R.B. Wahiddin, J. Mod. Opt. **44**, 1005 (1997).

[19] S. Smart and S. Swain, Phys. Rev. **A48**, R50 (1993).

[20] P. Zhou and S. Swain, Phys. Rev. **A55**, 772 (1997), and references therein.

[21] M. Bosticky, Z. Ficek and B.J. Dalton, Phys. Rev. **A53**, 4439 (1996).

[22] Z. Ficek and B.J. Dalton, Opt. Commun. **102**, 231 (1993).

[23] J.M. Courty and S. Reynaud, Europhys. Lett. **10**, 237 (1989).

[24] Z. Ficek, W.S. Smyth and S. Swain, Phys. Rev. **A52**, 4126 (1995).

[25] Z. Ficek and P.D. Drummond, Phys. Rev. **A43**, 6247, 6258 (1991).

[26] V. Buzek, P.L. Knight and I.K. Kudryavtsev, Phys. Rev. **A44**, 1931 (1991).

[27] Z. Ficek and P.D. Drummond, Europhys. Lett. **24**, 455 (1993).

[28] J. Gea-Banacloche, Phys. Rev. Lett. **62**, 1603 (1989).

[29] J. Javanainen and P.L. Gould, Phys. Rev. **A41**, 5088 (1990).

[30] N.Ph. Georgiades, E.S. Polzik, K. Edamatsu, H.J. Kimble and A.S. Parkins, Phys. Rev. Lett. **75**, 3426 (1995).

[31] N.Ph. Georgiades, E.S. Polzik and H.J. Kimble, Phys. Rev.**A55**, R1605 (1997).

Advanced Thin Films

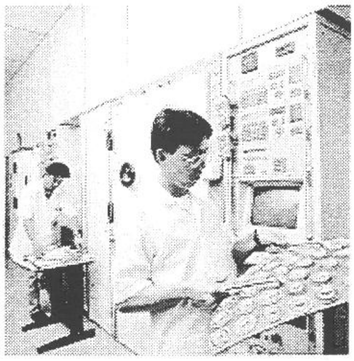

Coating applied using ion-assisted deposition (IAD) technology have advantages which will give your product the edge. Ions bombard the surface producing a dense film:

- High durability
- Consistent optical properties
- Smooth surface suitable for lasers

IAD produces tough films without the need to heat the substrate. Temperature sensitive materials can be coated :

- Plastics
- Infra-red optics
- Semiconductors
- Fire optics
- Large optics
- Crystalline material

Consult Avimo's staff to discuss how IAD can benefit your products

ATF 1000 Series Anti-reflection Coatings

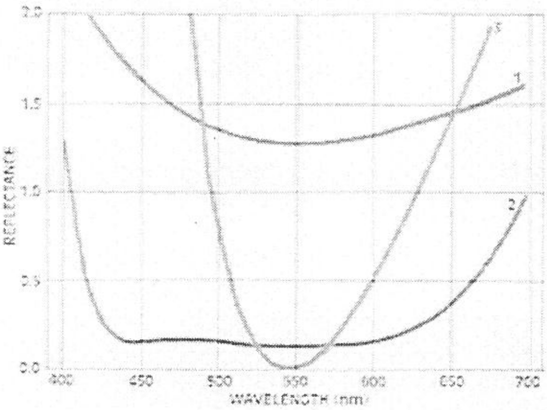

1. Single layer MgF_2; a historic standard.
2. Board band multilayer in the wavelength range of your choice.
3. V-coating; nearly zero reflectance at a specific wavelength.

ATF 1000 Series Metallic Coatings

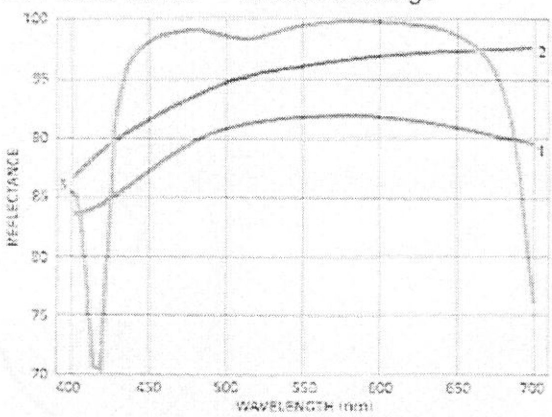

1. First surface aluminium protection with SiO_2.
2. First surface silver with multilayer protection.
3. Enhanced first surface aluminium.

Avimo metallic coatings are protected to withstand environmental extremes. Second surface reflective coatings are also available.

ATF 5000 Series Dielectric Edge Filters

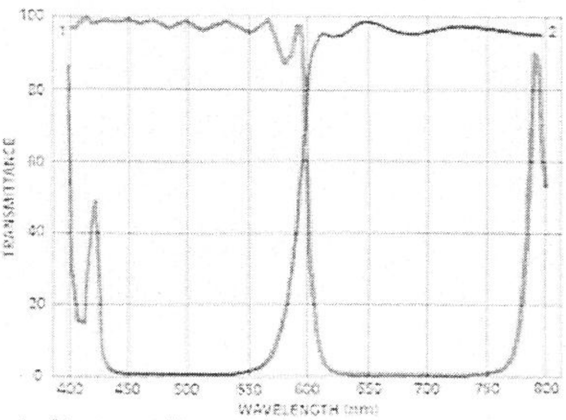

1. Short pass filter. 2. Long pass filter.

The primary wavelength, the slope of the edge, the blocking properties and the transmitting properties can all be designed and controlled to suit your requirements.

ATF 6000 Series Dielectric Bandpass Filters

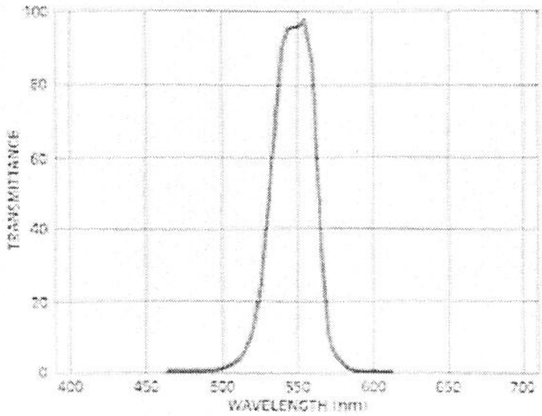

Avimo will design and produce filters to meet your requirements for central wavelength, the full width at half max and blocking properties.

As a "Center of Coating Excellence" for precision optics, Avimo has developed conventional physical vapor deposition as well as ion-assisted deposition (IAD) technology to produce high performance optical thin films. Choose from our lists of proven coating designs or have our thin film team design a coating to meet your specific needs. For further details, please contact :

Avimo Electro-Optics Pte Ltd
A Subsidiary of Avimo Group Ltd
14 Fifth Lokyang Road . Singapore 629763
Tel : 2655122 . Fax : 2651479 . E-mail : aeo@pacific.net.sg

AVIMO
ELECTRO-OPTICS PTE LTD

CSIRO Manufactures Optics for LIGO*

Chris Walsh
CSIRO Division of Telecommunications and Industrial Physics,
PO Box 218, Lindfield NSW 20270, Australia

*Based on work supported by NSF under contract PHY-9210038. Opinions, findings etc are those of the authors and do not reflect the view of NSF

Optics for the Laser Interferometer Gravitational Wave Observatory (LIGO) are being manufactured and tested by the optics group at the CSIRO Division of Telecommunications and Industrial Physics. The specifications and metrology required for these optics are discussed.

1. Introduction

One of the most prestigious optical fabrication contracts offered internationally has been won by an Australian group. Core optics for the Laser Interferometer Gravitational Wave Observatory (LIGO) are being manufactured and tested by the optics group at the CSIRO Division of Telecommunications and Industrial Physics (formerly Applied Physics). LIGO is a US$300M project funded by the US National Science Foundation and managed by the California Institute of Technology and Massachusets Institute of Technology[1]. Its purpose is to detect and measure gravitational waves through their interaction with 'test' masses which double as mirrors at the ends of a long path (≈ 4 km) interferometer. The weak interaction of the gravitational waves with the test masses produce small displacements of the mirrors (of order 10^{-9} of an atomic diameter!) which are detected as changes in the null fringe configuration of the interferometer.

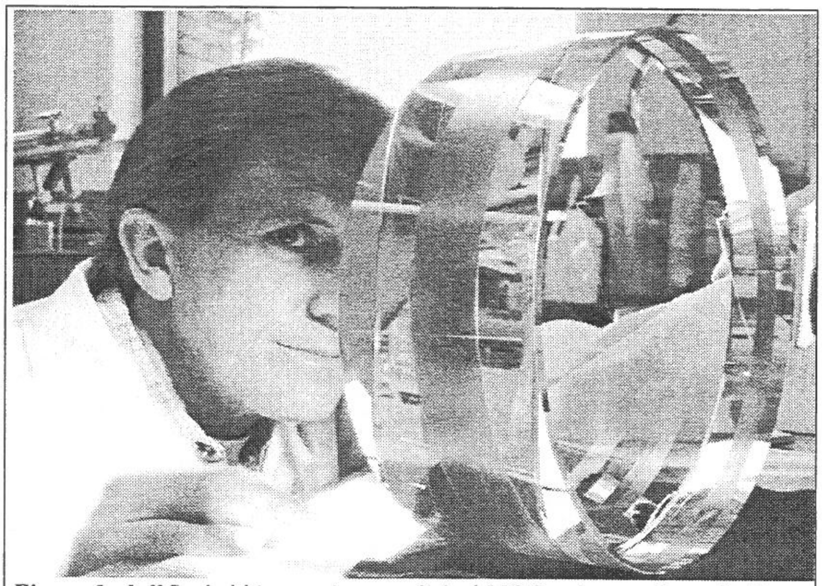

Figure 1: Jeff Seckold inspecting a polished LIGO substrate for polishing scrtaches or point defects

An example of the optical components being produced by CSIRO is shown in Figure 1. The material is the highest quality fused silica and comes from two vendors: Corning in the US and Heraeus in Germany (Heraeus is supplying a special low absorption glass required for key interferometer components where thermal lensing may occur).

The blanks alone have an average value of around $40,000 each. The optical finish required for these surfaces is at the very limits of current capabilities of optical fabrication and metrology, especially over such large apertures.

The process leading to the award of the contract to CSIRO took place in several stages. A feasibility stage (called Pathfinder) was first undertaken in which four vendors (including CSIRO) manufactured optical surfaces to specifications comparable to those for the final optics. CSIRO and another vendor, Hughes Danbury Optical Systems (HDOS), were also asked to provide measurement data on the optical surfaces. The next stage was an independent assessment of the surfaces by a metrology group at NIST Gaithersburg led by Chris Evans. The final stage was the tendering process for the final optics package "core optics"). Pathfinder was commenced in late 1995 and concluded in March 96. Tenders for the core optics package were called for in September 1996 and a contract award for twenty substrates was made to CSIRO in December 1996.

2. Pathfinder

Each optical substrate manufactured as part of the Pathfinder project had a concave surface of radius 6 km on one side and a nominally flat surface on the other side of a wedged cylindrical substrate made of high quality fused silica 250 mm diameter by 100 mm thick. The specifications for the surfaces can be summarised as follows:

- Power (after removing a 6 km sphere in the case of the curved surface) and astigmatism to be each less than $\lambda/20$ ($\lambda = 633$ nm)

- The standard deviation of the low frequency surface variations ('waviness') with piston, tilt, power and astigmatism removed (σ_L) to be less than $\lambda/800$ over the central 80 mm of each surface and $\lambda/400$ over the central 200 mm

- The rms of the surface errors in the high frequency band (σ_H) to be less than 0.4 nm.

To manufacture these optics the fabrication team, led by Achim Leistner and including Jeff Seckold, Peter Neuweger, Ron Bulla and Mark Suchting used the teflon lap polishing technique which has been used at CSIRO for many years to produce flat surfaces in a reproducible and deterministic manner. The method is described in detail elsewhere[2].

Teflon polishing possesses several advantages for work of this kind compared to pitch polishing. These can be summarised as follows:

- In Teflon laps a number of the important polishing parameters such as lap flatness and surface conditions, polishing agent and fluid composition can be predetermined. The classical pitch lap technique does not allow such a degree of control, because pitch flows and its surface properties may vary constantly during polishing.

- In-process measurements can be conveniently performed during the Teflon polishing process. The substrate can be removed from the lap, tested (a process which may take 24 hours for the highest precision measurements) and replaced on the lap without any changes occurring in the shape of the lap. Changes at the nanometre level will always occur on pitch laps because of the viscous nature of the material.

As an example of the benefits of teflon lap polishing, consider the production of the 6 km radius surface. The shape of this curve needs to be tuned to within $\lambda/20$ of the specification. We achieved this through an iterative process. The lap was first "conditioned" by mechanical abrasion with a fine ground silica plate. The surface of the lap can be curved to the correct radius in this way. The substrate is then polished on the lap and measured interferometricallly to obtain the figure and this information is fed back to recondition the lap towards the desired curvature. This process is possible on a teflon lap because of its mechanical rigidity, but not on pitch.

The measurements were carried out by a team including Chris Walsh, Bob Oreb and Dave Farrant, Achim Leistner and Mark Suchting, with valuable advice from 'Hari' Hariharan. We relied on two instruments to measure the final optics: a WYKO 6000 digital phase shifting interferometer to measure power, astigmatism and σ_L and a TOPO profiling microscope to measure σ_H. Although the measurements at the high spatial frequencies are well within the capabilities of the TOPO, the measurements of waviness (σ_L) to sub-nm levels of precision might appear at first glance to be beyond the capabilities of a conventional large aperture interferometer. In practice, however, we achieved this resolution.

The interferometer was operated in a metrology room separate from the manufacturing area with temperature and humidity control. An 8 bit digitising system gave a possible measurement resolution of around one nanometre at each of the 736 by 480 pixels. The principal environmental noise sources were air currents driven by acoustic sources and thermal gradients. Through careful attention to minimising effects due to air turbulence, we found that the difference phase map between any two sets of measurements (each an average of between 10 and 20 measurements) had an rms error

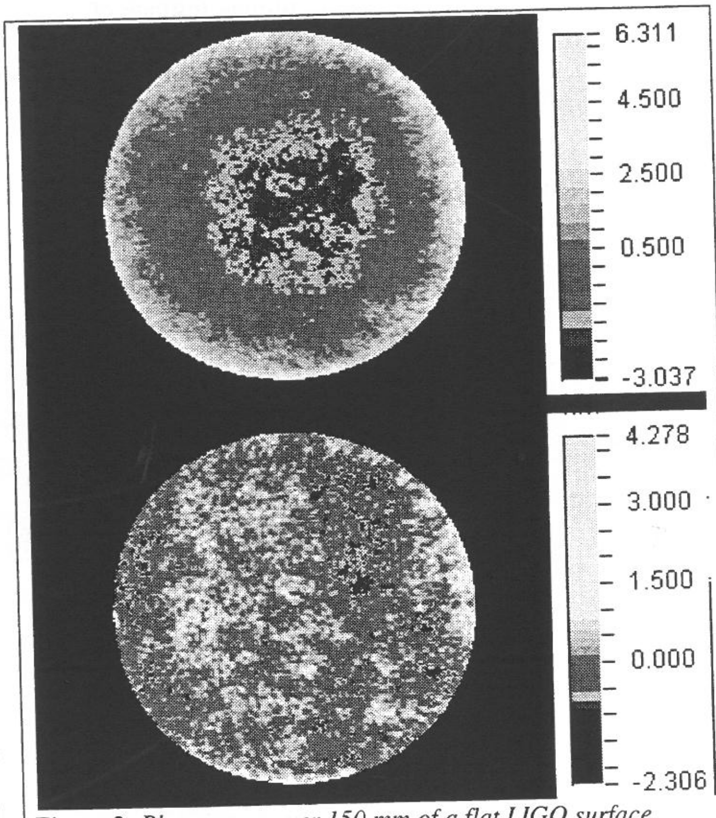

Figure 2: *Phase maps over 150 mm of a flat LIGO surface without (top) and with (below) power and astigmatism removed. The scale on the right is in nanometres.*

less than 0.35 nm over the 150 mm aperture.

A phase map of a nominally flat surface with the effects of the reference surface removed, so that it represents to a good approximation the shape of the flat LIGO surface, is shown in Figure 2.

The small amount of power and astigmatism seen in the map at the top (less than 0.01 waves) has been removed in the lower map. The deviations from a plane surface seen in this phase map have an RMS error of 0.4 nm or better than $\lambda/1000$ over the 150 mm aperture, comfortably within the LIGO specification.

Measuring the curved surfaces against a flat reference introduces systematic errors which ruin any accurate estimate of σ_L. These include retrace errors in the interferometer as well as errors associated with fringe vibration (due to turbulence etc) that appear once the interferometer no longer operates at a null fringe. The only way to eliminate these errors is to again set up a null fringe interferometer. For testing a concave surface, this means a convex reference surface is required. Remarkably, Achim and Mark succeeded in fabricating such a surface, which matched the concave 6 km surface to within a thirtieth of a wave in power! Once we had this surface, testing of the curved surface was possible. The radius of curvature was still measured against an absolutely calibrated flat reference. Our error budget for this measurement was ± 100 metres in a radius of 6 km, or about $\pm\lambda/40$ in power.

3. Core Optics

In the Pathfinder project we demonstrated that CSIRO had both the fabrication and metrology capability for the project by producing and measuring surfaces to the LIGO specification. At present we are working on the core optics package; after coating at Research Electro Optics (REO) in Boulder, these optics will be installed in the LIGO observatories in Washington State and Lousianna. A full description of the optical system in LIGO is beyond the scope of this article, and the reader is encouraged to visit the LIGO web site[1] for more information.

CSIRO is manufacturing 20 optical substrates, comprising 4 folding mirrors, 4 end test masses, 7 recycling mirrors and 5 beamsplitters. The first set of optics to be completed (the folding mirrors) were shipped in July and the next set (the end test masses) are to be shipped by the end of August. The completion of all the optics is scheduled for the second quarter of 1998.

Acknowledgements

CSIRO has been active in research and development of optical fabrication and metrology techniques for many years, and the award of a contract of this kind is welcome recognition for our international standing in this area. However, international standing alone is often insufficient and it is a pleasure to acknowledge the collaboration and good words said on our behalf by our colleagues in the Australian Consortium for International Gravitational Astronomy (ACIGA), who have constantly reminded their international collaborators of our skills and capabilities.

References

[1]. See the LIGO web site at http://www.ligo.caltech.edu for more information

[2]. For references on teflon polishing, see Leistner, A. J., Thwaite, E. G., Lesha, F., Bennett, J. M., "Polishing study using Teflon and pitch laps to produce flat and supersmooth surfaces," Appl. Opt. **31**, 1472-1482 (1992).

Turn on the sun with an Oriel Solar Simulator

If you need to closely simulate the sun's spectrum for environmental studies, cosmetics/dermatology testing, and photodegredation studies, aside from the real thing, there's nothing better than an Oriel Solar Simulator.

Oriel offer full spectrum simulators to match various Air Mass (AM) conditions and UV models that simulate the UV portion only (radiation < 400 nm) of the solar spectrum. All Oriel solar simulators come with ozone free xenon arc lamps, of corresponding power tot he simulator, which emit radiation down to ~260 nm. Oriel also off lamps that emit to 220 nm. Oriel's 1000 Watt Solar Simulators come in four different output assemblies to produce 2 x 2, 4 x 4 6 x 6 and 8 x 8 inch uniform collimated beams. Larger beam sizes for illuminating larger areas are also available. 300 Watt sources produce a uniform collimated 2 x 2 inch output beam with power equivalent to 2 suns. The economical 150 Watt Solar Simulator's small arc size allows you to efficiently focus the light onto a fibre optic or liquid light guide.

Fibre and Waveguide Characterisation Beyond the Diffraction Limit

Shane T Huntington, K. A. Nugent, A. Roberts, P. Mulvaney, K. M. Lo# and M. Bazylenko†*

*School of Physics (*School of Chemistry), University of Melbourne, Parkville, 3052.*
#Dep. of Electrical and Electronic Engineering, University of Hong Kong, Pokfulan Road, Hong Kong.
†School of Electrical Engineering, The University of New South Wales, Sydney, 2052.

The guiding properties and refractive index profiles of optical waveguides are usually measured using conventional optical systems. These systems are limited by diffraction to a resolution of about 300 nm. We use atomic force microscopy and near-field microscopy to reach beyond this limit.

1. Introduction

Over the past ten years, optical fibres have found applications in a vast number of areas. These applications include high-speed communications, light delivery systems, and sensors for a wide range of quantities (such as mechanical strain and solution concentration). As applications become more and more demanding, the accurate characterisation of optical fibres becomes critical. Both the guiding properties and the refractive index profiles of fibres are generally measured using conventional optical systems. These systems are diffraction limited (to about 300nm, depending on the wavelength) and as a result, cannot be used to accurately determine fibre parameters.

Two important features of any waveguide are the refractive index profile (the structure of the waveguide), and the mode profile (the shape of the light which propagates in the waveguide). We use two high resolution techniques — atomic force microscopy and near-field microscopy — to investigate these profiles with high accuracy.

1.1 Atomic Force Microscopy

To measure the refractive index profile of a waveguide we use a novel technique based on a combination of etching and Atomic Force Microscopy (AFM). This technique may be applied to optical fibres and also to waveguides fabricated using PECVD [1-3]. The validity of the technique is addressed and typical profiles for an elliptical core fibre, twin core fibre and PECVD waveguides are presented. The lateral resolution of this technique is limited only by the resolution of the AFM tip, typically less than 3nm for this work. It should be noted that conventional techniques for fibre profiling have a resolution limit of about 500nm. As a consequence it is quite common to profile the fibre preform prior to drawing and then assume that the refractive index profile scales as the fibre outer diameter. This method of circumventing the diffraction limit is indirect and does not include the drawing process as a possible contributing factor to the final fibre index profile.

1.2 Near Field Scanning Optical Microscopy

Almost seventy years ago, E. H. Synge [4] proposed a method of imaging where the limitations of optical microscopy would be absent, but at the same time all the advantages of conventional optical microscopy would be retained. The first microscope of this type, known today as a Near Field Scanning Optical Microscope, was constructed in 1984, some fifty-six years after the concept was first reported. Since then the technique has not only gained popularity in itself but has spawned advances in other areas of microscopy as well.

Near Field Scanning Optical Microscopy (NSOM) breaks the diffraction barrier by scanning a sub-wavelength aperture across a sample. The absence of any lensing apparatus means that the resolution is determined solely by aperture size and working distance. Today there are a number of different "probes" being used in near field microscopy, but the most popular by far is the optical fibre probe. In this case the probe is fabricated by heating and drawing an optical fibre until it breaks. The sides of the fibre are then coated to make them opaque, leaving a sub-wavelength aperture at the very tip [5] (see figure 1).

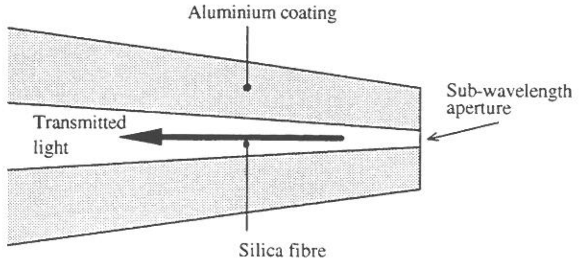

Figure 1: *Schematic of a NSOM probe fabricated from single mode optical fibre.*

In the second half of this article we discuss the use of NSOM to measure the field of a specific fibre — the "D" fibre [6-8]. The evanescent fields surrounding D-shaped optical fibres is measured directly and compared to theoretical expectations. The mode profile of the D-fibre is also measured.

2. Refractive Index Profiling with AFM Resolution

There are a number of techniques for the determination of refractive index profiles, and all have some disadvantages. Optical fibres can be examined either before or after the drawing process. If the profile is determined from the preform then any changes that may occur during the drawing process are unknown. On the other hand, if the drawn fibre is examined optically, the data will have poor resolution due to the constraints imposed by the diffraction limit.

We have developed a new technique that combines etching and atomic force microscopy to obtain index profiles with unprecedented resolution — directly from drawn fibres. The etch rate for silica is dependent on the dopant and its concentration. By etching a cleaved fibre endface in HF and measuring the resulting topography, the location and concentration of dopants can be ascertained. Since the refractive index is determined by these quanitities, the AFM images can be used to determine the refractive index profile. This technique is not restricted to optical fibres with simple geometries; it can just as easily be used on multiple core fibres and buried channel waveguides, regardless of their complexity.

2.1 Validity of the AFM/Etching Technique

If the AFM/etching technique is to be used to characterise fibres and waveguides, it is first necessary to determine whether or not the profiles are dependent on the etching process itself. To this end, ten single mode optical fibres were etched for a variety of times ranging from 0 to 3 minutes in 5% HF. The resulting AFM profiles are shown in Figure 2.

Several parameters have been selected from Figure 2 to allow the profiles to be examined quantitatively. The parameters labelled A and B allow the lateral geometry of the fibre to be examined, whereas parameters C and D represent the vertical geometry (or height). Measurements of A and B show that they are consistant for all samples, regardless of the etch time. The mean value for A was 2.56 ± 0.03µm and the mean for B, 4.49 ± 0.07µm. This indicates that the lateral features are independent of the etch time. The vertical parameters C and D are plotted against etch time in Figure 3. The linear relationship between etch time and etch depth implies that the etch rate depends only on the local fibre composition.

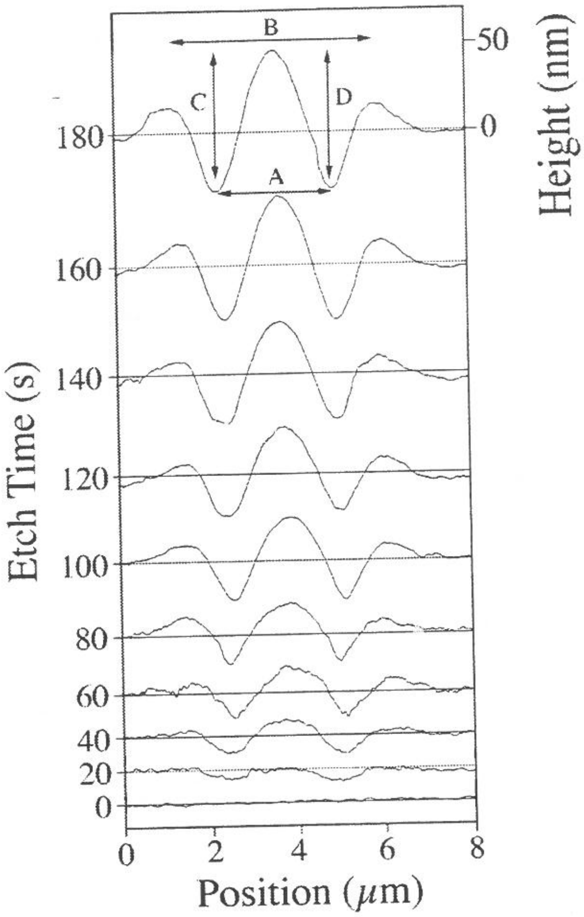

Figure 2: *AFM/etching profiles for ten fibres with etch times ranging between 0 and 3 minutes.*

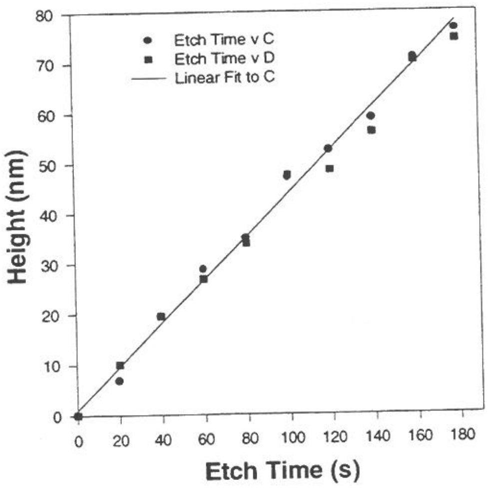

Figure 3: *Plot of etch depth vs etch time for a single mode optical fibre.*

The profiles obtained for fibres that contain only a single dopant species can be scaled linearly to refractive index. If there are a number of dopants present, the analysis of the etched topography is more complex. Such fibres could be profiled using multiple etchants specifically chosen so that the various components could be decoupled.

The AFM phenomenon known as “tip convolution”, in which the image is the convolution of the imaging tip and the sample itself, must also be considered. This effect, due to self-imaging of the tip/cantilever, can cause distortions in the data obtained by the AFM. It is a consequence of the fact that the resolution of the AFM is limited by the tip size and shape. This type of problem is usually only observed when objects that are of similar size to the tip itself are examined or when very deep and sharp depressions in surface topography are present. The samples examined here exhibit neither of these features and thus tip convolution was not observed in any of the fibre or waveguide measurements. We thus conclude that the AFM/etching technique is an accurate method of profiling fibre structure with nanometric resolution.

2.2 The Elliptical Core Fibre

The elliptical core fibre was chosen as a challenging test sample due to its small core size and inherent asymmetry. In addition, detailed preform data was available [9] on this fibre (OFTC AD023-05). The fibre was stripped, cleaved, and etched for 40 seconds in 5% HF solution. Figure 4 below shows a typical image of the elliptical core fibre endface as measured by the AFM in contact mode. This fibre has a germanium doped core that appears depressed in the image.

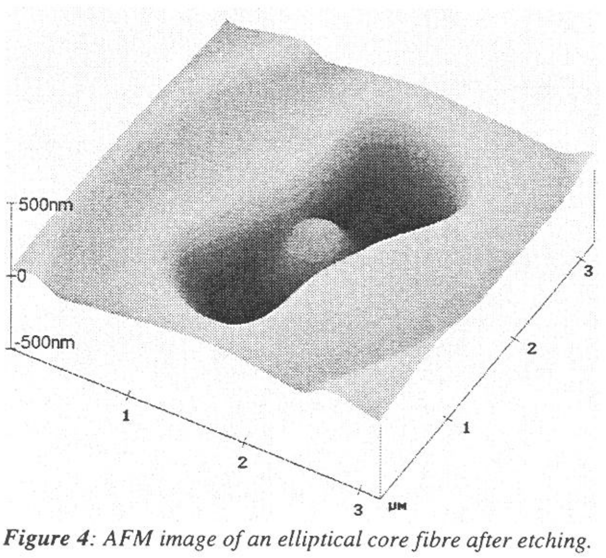

Figure 4: AFM image of an elliptical core fibre after etching.

In Figure 5 the preform profiles in the x and y directions are compared to those obtained by the AFM. The preform data needs to be scaled down to match the drawn fibre size. In this case the scaling has been done so that the preform major axis profile matches the AFM major axis profile. When this is done there is a noticable discrepancy between the minor axis profiles. This indicates that the fibre parameters are changing during the drawing process and thus it must be concluded that for this fibre the preform index data cannot be used to infer the index profile of the drawn fibre.

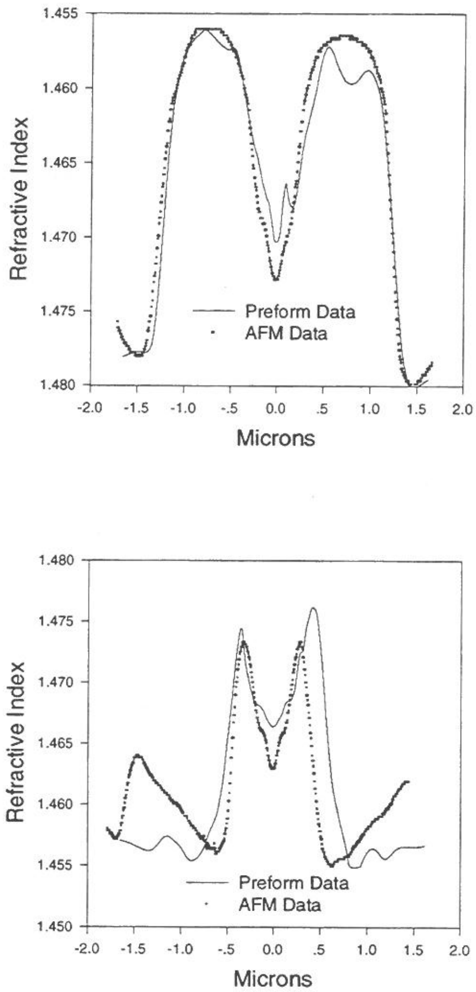

Figure 5: Major axis (above) and minor axis (below) profiles for the elliptical core fibre as measured from the preform and drawn fibre.

2.3 Twin Elliptical Core Fibre

To demonstrate the versatility of the AFM/etching technique, a twin core fibre has also been profiled. Figure 6 shows an AFM image of the Twin Elliptical Core Fibre after etching for 30 seconds in 10% HF solution. Note that in this case the cores were imaged collectively. This limits the resolution of the AFM to about 50nm. If a higher resolution is required the cores can be easily examined individually.

A profile of the two fibre cores is shown in Figure 7. Again the higher index regions (doped silica) are etched at a faster rate than the surrounding cladding. The depressions therefore represent regions of enhanced refractive index.

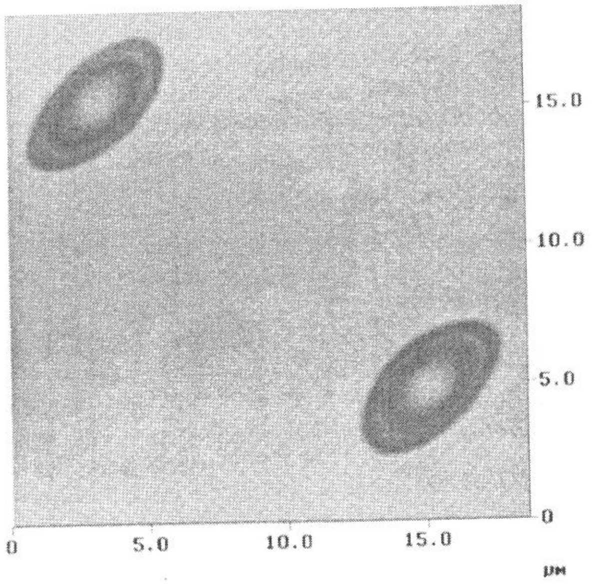

Figure 6: AFM profile of an etched Twin Elliptical Core Fibre.

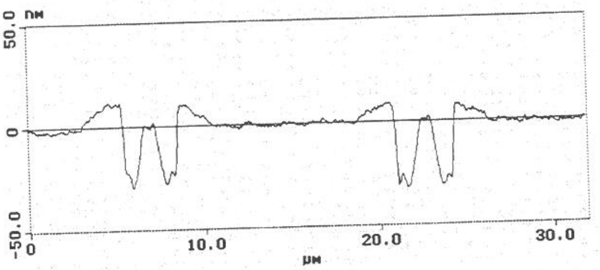

Figure 7: Cross section of the twin core fibre image showing both cores simultaneously.

2.3 Buried Channel Waveguides

The AFM/etching technique is not limited to optical fibres: buried channel waveguides can also easily be examined. These waveguides are fabricated using PECVD on silicon substrates [10]. Figure 8 shows an AFM height profile of a germanium doped buried channel waveguide after etching in 5% HF solution for 1 minute.

A number of features of interest are visible in this image. The germanium doped guiding region is labelled A. The lower silica cladding is labelled B and the upper silica cladding is labelled C. The line at D represents the connection between the upper and lower cladding layers which are deposited separately. At E there is a 'seam' like structure that is apparent on both sides of the guide. This structural feature is the result of the connection of two growing surfaces during the deposition of the upper cladding onto the surface of the buffer layer and the sidewalls of the core. At point F there is a dip in the profile caused by a local increase in the germanium doping. This is a result of an initial pulse in the GeH_4 flow during deposition. Point G represents the top surface of the waveguide. (We note that some of the features detected by our technique have little effect on the optical behaviour of the device, but lead to the enhancement of the fabrication process.)

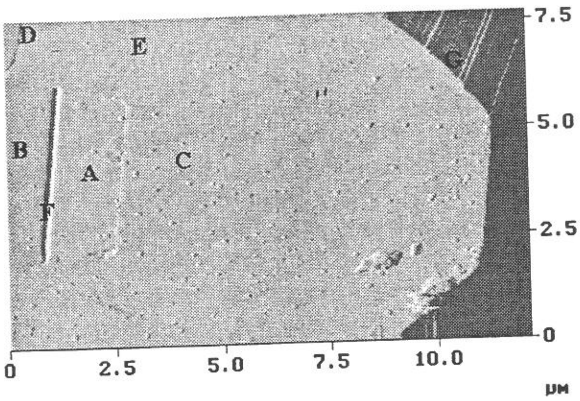

Figure 8: AFM image of a PECVD Buried Channel Waveguide after etching.

The acquisition of accurate fibre information is essential to facilitate modelling and to optimise fibre performance. When comparing theoretical field calculations with measured ones, preform data is often not enough to obtain a good correlation. Diffraction-limited data obtained by measuring the drawn fibre with conventional optical techniques is also inadequate. The AFM data, on the other hand, has superior resolution to the conventional measurements and can therefore be used in accurate calculations of the fibre fields.

3. The D-Shaped Optical Fibre

We now turn to the investigation of the fields around fibres and waveguides. A particularly interesting example is the field around a "D-Fibre". This fibre is identical to a standard single mode fibre with the exception that the cladding is D shaped. This places the core of the fibre within just a few microns of the cladding/air interface, as shown in Figure 9.

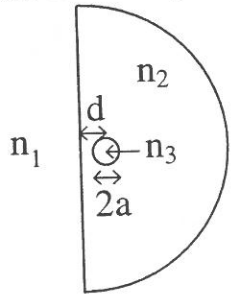

Figure 9: Cross section of D-shaped optical fibre .

The proximity of the core to the interface means that there will be some component of the evanescent field outside the fibre. This field, although propagating almost unchanged along the fibre, decays exponentially with lateral distance from the core. Because part of the field sits outside the fibre, the overall transmission depends on the external environment. When used as a sensor [11], the D-fibre can be placed within environments that couple power out of the fibre. Power fluctuations are measured and information about changes to the environment can be inferred. As is the case for all optical fibres, the D-fibre is chemically inert and can be placed in environments that are hostile to other sensors. In addition, optical transmission rates allow for much better temporal resolution than electrically driven sensors. The D-fibre therefore represents a superior alternative to its electronic counterparts.

3.1. Locating and Profiling the Core

Before the D-fibre can be modelled, parameters such as the core's shape, profile, size and distance from the cladding/air interface must be determined. In order to obtain this information our technique using the Atomic Force Microscope is used. Initially the D-fibre is precision cleaved and the endface is exposed to 5% HF solution for 1 minute. The core of the fibre is germanium doped and as a result it has an enhanced etch rate compared to the pure silica cladding. Once appropriately mounted, the fibre is examined under an Atomic Force Microscope.

Figure 10 shows an example of a typical AFM image of the D-shaped optical fibre. From this topographical image the core details and core to cladding/air interface distance can be accurately determined. Figure 11 shows a cross section of the core region of this image. Since the germanium doped regions have a higher refractive index and etch rate than the silica cladding, a peak in the AFM profile represents a depression in the refractive index profile. The lateral resolution of this technique is of order 1nm.

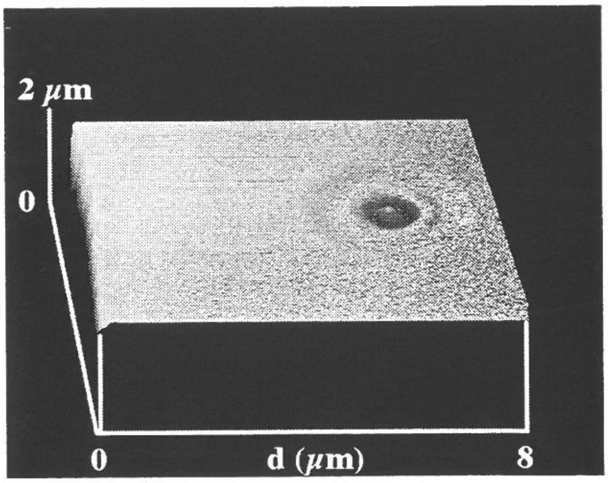

Figure 10: AFM image of the endface of an etched D-shaped optical fibre showing core and cladding edge.

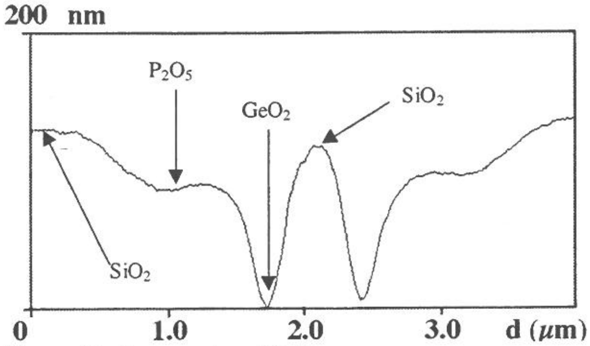

Figure 11: Cross section of D-fibre core

3.2. Modeling the D-fibre

The field properties of the fibre are determined using a Point Matching Method [12]. This models the fibre by assuming that it has a circular core comprised of a radially varying refractive index profile (as is indeed the case). The air closest to the fibre core is approximated by a circular air side-pit that has a radius four times that of the core (the minimum required for convergence). This method entails the expansion of the electromagnetic field in terms of a series of Bessel and modified Bessel functions that are multiplied by trigonometric functions. The fields within the core are then equated to the fields inside the cladding at selected points along the core/cladding boundary. The resulting equations are solved numerically.

3.3. Evanescent Field Measurements

As discussed above, the near field microscope is able to measure evanescent fields directly. Near field probes are, therefore, an ideal tool for the characterisation of the non-propagating fields. In these experiments the D-shaped fibre fields are measured with sub-wavelength resolution and compared to theoretical predictions.

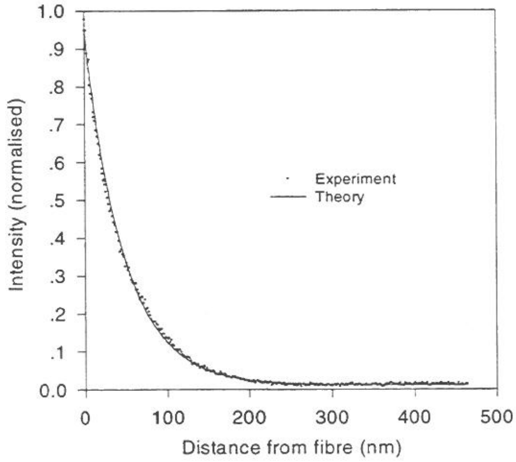

Figure 12: Evanescent field plot for the D-shaped optical fibre.

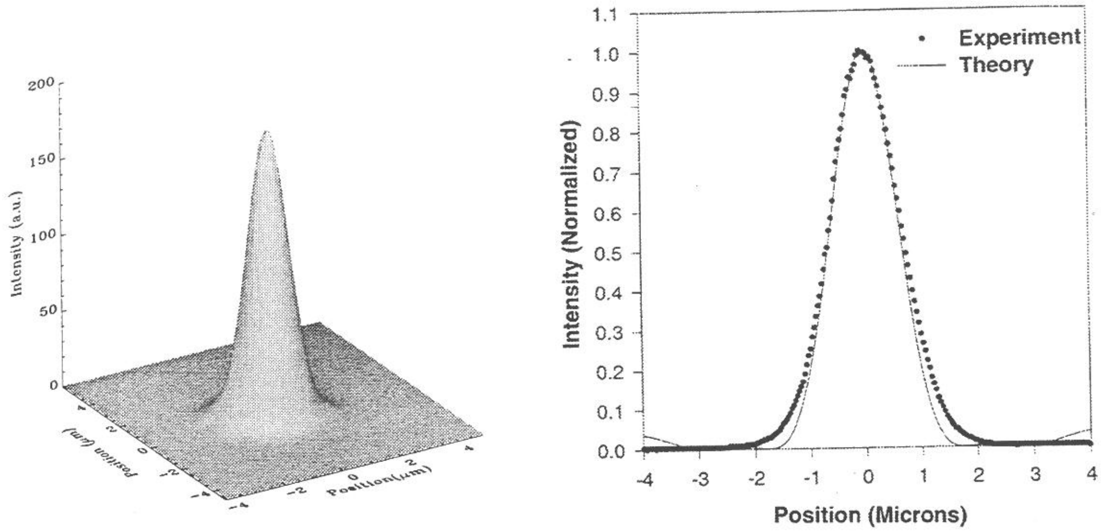

(a) (b)

Figure 13: *(a) 2D surface plot of the mode field pattern at the end of a D-shaped optical fibre, (b) Comparison between theoretical and experimental cross sections for the mode pattern shown in (a).*

Figure 12 shows a 256 point scan of the region beyond the cladding/air interface of the D-fibre. The measured exponential decay constant for the field is $0.0213 \pm 0.0001 nm^{-1}$. The theoretical decay constant for this fibre is $0.02109 nm^{-1}$, which is in excellent agreement with experiment.

3.4. Mode Field Measurements

The near field microscope can be used to measure the mode field at the end of the D-fibre. Figure 13a shows a 256x256 point scan at a working distance of less than 500nm. At this distance the measured profile is a good approximation to the mode profile at the fibre endface. This method of determining the mode profile of an optical fibre using NSOM has been shown to yield accurate results with a resolution far exceeding conventional "far field" microscopy [8]. Figure 13a is a surface plot of the raw data, illustrating the low noise of the system. Figure 13b is a cross section of figure 13a in the x direction with the corresponding theoretical prediction. The measured mode field radius is 1.234 ± 0.007 μm and the predicted value is 1.115 μm. There is a slight discrepancy between the predicted and measured profiles. This may be caused by the fact that the model assumes the mode is polarised in one direction, but this is not the case in the experiment.

4. Conclusions

The combination of Near Field Scanning Optical Microscopy and Atomic Force Microscopy allows optical fibres and waveguides to be examined with resolution well beyond the diffraction limit. Near field imaging offers the advantage of direct evanescent field detection in addition to sub-wavelength resolution. AFM/etching allows the refractive index profiles of optical fibres and waveguides to be measured with resolution that is only limited by the AFM tip radius — typically 3nm for this study [13].

Acknowledgments

The authors wish to acknowledge the support of the Australian Research Council. S.T.H acknowledges the support of a University of Melbourne Teaching and Research Award. P.M. acknowledges receipt of an ARC QEII Fellowship and the financial support of the Advanced Mineral Products Research Centre, an ARC Special Research Centre. We also acknowledge the Optical Fibre Technology Centre, Sydney, for providing us with the elliptical core fibre, and in particular Ron Bailey for profiling our fibre with the York P102 preform profiler. The Twin Elliptical Core Fibre was supplied by John Arkwright (UNSW). Finally, we thank Marcy Faith, Ian Bassett, John Love and the members of the Australian Photonics Cooperative Research Centre for their insightful discussions.

References

[1]. Q. Zhong and D. Inniss, J. Lightwave. Technol. **12**, pp.1517-23 (1994).

[2]. S. T. Huntington, K. A. Nugent, A. Roberts, K. M. Lo and P. Mulvaney, J. Appl. Phys., **82** (2), pp.510-513 (1997).

[3]. S. T. Huntington, P. Mulvaney, A. Roberts, K. A. Nugent and M. Bazylenko, J. Appl. Phys, **82** (6), 15th Sept (1997).

[4]. E. H. Synge, "A suggested method of extending microscopic resolution into the ultramicroscopic region", Phil. Mag., **6**, p.356 (1928).

[5]. E. Betzig and J. K. Trautman, Science **257**, pp189-95 (1992).

[6]. D.J Butler, K.A. Nugent and A. Roberts, J. Appl. Phys. **75**(6), pp.2753-56 (1994).

[7]. J. K. Trautman, E. Betzig, J. S. Weiner, D. J. DiGiovanni, T. D. Harris and F. Hellman, J. Appl. Phys. **71**, pp.4659-63 (1992).

[8]. D.J.Butler, A.Horsfall, K.A.Nugent, A.Roberts J.Appl.Phys. **77** (11) pp5514-5517 (1995)

[9]. D. J. Butler, A. Horsfall, K.A. Nugent, A. Roberts, I.M. Bassett and K.M. Lo, J. Appl. Phys. **77** (11), pp.5514-5517 (1995).

[10]. M. V. Bazylenko, M. Gross, P. M. Allen and P. L. Chu, IEEE Photonics Technology Letters, **7**, (7), pp.774-776 (1995).

[11]. F. A. Muhammad and G. Stewart, Electron. Lett, **28**, pp.1205-6 (1992).

[12]. E. Yamashita and K. Atsuki, "The Point Matching Method," in Analysis Methods for Electromagnetic Wave Problems, edited by E. Yamashita (Artech, Boston, 1990), Chap.3

[13]. P. Mulvaney and M. Giersig, J.C.S. Fara. Trans. **92**, pp.3137-3143 (1996).

SUDDENLY, NASA LOSES CONTROL OF THE MARS ROVER...

Meetings Calendar at a Glance

Date	Meeting	Contact	Location
	1997		
Sep 5-9	Biomedical Optics Europe V	EOS	San Remo, Italy
Sep 6-8	COLOQ'97	EOS	Strasbourg, France
Sep 9-12	5th International Conference on Optics (ROMOPTO'97)	EOS	Bucharest, Romania
Sep 13-18	Quantum optics	OSA	Castelv. Pascoli, Italy
Sep 15-17	FRINGE '97 Automatic Processing of Fringe Patterns	SPIE	Bremen, FRG
Sep 17-19	Photomask Technology and Management	SPIE	Santa Clara, California
Sep 21-25	European Symposium on Satellite Remote Sensing IV	EOS	London, United Kingdom
Sep 22-26	Atomic and Molecular Pulsed Lasers II	SPIE	Tomsk, Russia
Sep 22-24	Photonics East and Electronic Imaging International	SPIE	Boston, Massachusetts
Sep 22-25	Integrated Optics and Optical Fiber Communications (IOOC '97)	OSA	Edinburgh, United Kingdom
Sep 22-25	European Conference On Optical Communication (ECOC'97)	OSA	Edinburgh, United Kingdom
Sep 29-30	Micromaching and Microfabrication	SPIE	Austin, Texas
Oct 1-3	Microelectronic Manufacturing	SPIE	Austin, Texas
Oct 6-8	Optical Materials for High Power Lasers	SPIE	Boulder, Colorado
Oct 12-17	OSA'97 Annual Meeting: Focus on the Life Sciences	OSA	Long Beach, California
Oct 12-17	Interdisciplinary Laser Science Conference (ILS-XIII)	OSA	Long Beach, California
Oct 15-17	Applied Imagery Pattern Recognition Workshop	SPIE	Washington, DC
Oct 15-17	Organic Thin Films For Photonics Applications Topical Meeting	OSA	Long Beach, California
Oct 17-18	Lasers In Dermatology: Bio-Optics and Treatment Of Human Skin	OSA	Long Beach, California
Oct 25-31	Fall Topical Meetings	OSA	Williamsburg, Virginia
Oct 25-31	12th International Conference on Optical Fiber Sensors	OSA	Williamsburg, Virginia
Oct 25-31	Glass and Optical Materials Division (GOMD) Meeting	OSA	Williamsburg, Virginia
Oct 25-31	Bragg Gratings, Photosensitivity, and Poling in Glass Waveguides	OSA	Williamsburg, Virginia
Oct 27-31	Joint Magneto-Optical Recording International Symposium (MORIS)	OSA	Yamagata, Japan
Oct 27-31	International Symposium On Optical Memory (ISOM '97)	OSA	Yamagata, Japan
Nov 17-20	Int. Congress on Applications of Lasers and Electro-Optics	OSA	San Diego, California
Nov 17-20	Color Imaging Conference: Color Science, Systems and Applications	OSA	Scottsdale, Arizona
Dec 4-6	DICTA-97 (Digital Image Computing: Techniques and Applications)		Auckland, New Zealand
Dec 4-6	Image and Vision Computing New Zealand		Auckland, New Zealand
Dec 10-12	AOS XI : The Bi-Annual Conference of the Australian Optical Society	AOS	Adelaide, Australia
Date	**Meeting — 1998**	**Contact**	**Location**
Jan 24-30	Photonics West	SPIE	San Jose, California
Feb 2-4	Advanced Solid-State Lasers Topical Meeting	OSA	Coeur D'Alene, Idaho
Feb 6-9	Vision Science and Its Applications Topical Meeting	OSA	Santa Fe, New Mexico
Feb 21-28	SPIE's International Symposium on Medical Imaging	SPIE	San Diego, California
Feb 22-27	Optical Fiber Communication Conference (OFC '98)	OSA	San Jose, California
Mar 9-13	Laser Applications To Chemical and Environmental Analysis	OSA	Orlando, Florida
Mar 9-13	Biomedical Topical Meetings	OSA	Orlando, Florida
Mar 23-27	Symposium on Advanced Networks and Imaging Technologies II	EOS	United Kingdom
Mar 30-3	Integrated Photonics Research	OSA	Victoria, Canada
Apr 1-3	Nonlinear Guided Waves and Their Applications	OSA	Victoria, Canada
Apr 16-17	Photomask Japan '98	SPIE	Kawasaki City, Japan
Apr 26-30	High Power Laser Ablation	SPIE	Santa Fe, New Mexico
May 3-8	Conference On Lasers and Electro-Optics (CLEO '98)	OSA	San Francisco, California
May 3-8	International Quantum Electronics Conference (IQEC '98)	OSA	San Francisco, California
May 10-13	Optical Data Storage	OSA	Aspen, Colorado
Jun 7-12	Optical Interference Coatings	OSA	Tucson, Arizona
Jun 8-11	OSA Summer Topical Meetings	OSA	Kailua-Kona, Hawaii
Jun 8-11	Diffractive Optics and Micro-Optics	OSA	Kailua-Kona, Hawaii
Jun 8-12	International Optical Design Conference	SPIE	Kailua-Kona, Hawaii
Jun 8-12	European Symposium on Environmental Sensing IV	EOS	Lyon, France
Jun 22-26	9th Conference on Laser Optics (LO'98)	SPIE	St.Petersburg, Russia
Jun 29-3	XVI International Conference on Coherent and Nonlinear Optics	SPIE	Moscow, Russia
July 13-16	International Symposium on Lasers and Materials	SPIE	Québec City, Canada
July 13-15	Photonics Taiwan: Asia Pacific Symposium on Optoelectronics	SPIE	Taipei, Taiwan China

Meetings Calendar at a Glance

July 19-24	SPIE's 1998 Annual Meeting	SPIE	San Diego, California
July 27-30	Conference on Applications of Photonic Technology	SPIE	Ottawa, Ontario, Canada
Sep 8-12	BiOS Europe '98 - European Biomedical Optics Week	EOS	Scandinavia
Sep 13-18	CLEO/Europe	OSA	Glasgow, Scotland
Sep 13-18	European Quantum Electronics Conference (EQEC '98)	OSA	Glasgow, Scotland
Sep 14-17	Remote Sensing: Atmospheric, Environmental, and Space	SPIE	Beijing, China
Sep 15-19	Congress on High-Speed Photography and Photonics	SPIE	Moscow, Russia
Sep 16-18	Photomask Santa Clara '98	SPIE	Santa Clara, California
Sep 21-25	European Symposium on Satellite Remote Sensing V	EOS	TBA, The Netherlands
Oct ?-?	Photonics Europe'98	EOS	Paris, France
Oct ?-?	Symp. on Optics and optoelectronics for Public Safety III	EOS	Paris, France
Oct ?-?	Symp. on Lasers, Optics and Vision for Productivity in Man. III	EOS	Paris, France
Oct 4-9	OSA Annual Meeting	OSA	Baltimore, Maryland
Oct 4-9	Interdisciplinary Laser Science Conference (ILS-XIV)	OSA	Baltimore, Maryland
Oct 14-17	Intelligent Systems and Advanced Manufacturing	SPIE	Pittsburgh
Nov 1-6	Photonics East	SPIE	Boston, Massachusetts
Date	**Meeting 1999**	**Contact**	**Location**
Feb 21-26	International Conference On Integrated Optics (IOOC '99)	OSA	San Diego, California
Feb 21-26	Optical Fiber Communication Conference (OFC '99)	OSA	San Diego, California
May 23-28	Conference On Lasers and Electro-Optics (CLEO '99)	OSA	Baltimore, Maryland
May 23-28	Quantum Electronics and Laser Science Conference (QELS '99)	OSA	Baltimore, Maryland
Sep 26-1	OSA Annual Meeting	OSA	Santa Clara, California
Sep 25-1	Interdisciplinary Laser Science Conference (ILS-XV)	OSA	Santa Clara, California
Date	**Meeting 2000**	**Contact**	**Location**
Mar 5-10	Optical Fiber Communication Conference (OFC 2000)	OSA	Baltimore, Maryland
May 7-12	Conference On Lasers and Electro-Optics (CLEO 2000)	OSA	San Francisco, California
May 7-12	Quantum Electronics and Laser Science Conference (QELS 2000)	OSA	San Francisco, California
Date	**Meeting 2001**	**Contact**	**Location**
Feb 18-23	Optical Fiber Communication (OFC 2001)	OSA	San Francisco, California
May 6-11	Conference On Lasers and Electro-Optics (CLEO 2001)	OSA	Baltimore, Maryland
May 6-11	Quantum Electronics and Laser Science Conference (QELS 2001)	OSA	Baltimore, Maryland

This list of optics related conferences is compiled from several sources and should be used as a guide only. Further information can be obtained from :

OSA
2010 Massachusetts Ave
NW Washington DC 20036
USA
Tel: +1 202 223 0920
Fax: +1 202 416 6100
Email: confserv@osa.org
http://www.osa.org/

SPIE
PO Box 10, Bellingham
WA 98227-0010
USA
Tel: +1 360 676 3290
Fax: +1 360 647 1445
Email : spie@mom.spie.org
http://www.spie.org/

EOS (attn. F. Chavel)
Centre Universitaire - B t. 503
B.P. 147 - 91403 ORSAY cedex -
France
Tel: +33 1 69 35 87 20
Fax: +33 1 69 85 35 65
Email : francoise.chavel@iota.u-psud.fr
http://www-eos.unine.ch/welcome/

AOS XI

The Eleventh Conference of the Australian Optical Society

The University of Adelaide, 10-12 December 1997.

High Average Power UV Sources Based on Copper Vapour Lasers

Daniel J W Brown
Centre for Lasers and Applications, Macquarie University
Sydney NSW 2109 Australia

High power UV lasers are highly sought after for applications in micromachining, photolithography and fluorescence mapping. Recent progress in nonlinear frequency conversion of the output of copper vapour lasers enables these sources to produce high average power (multi-watt) UV at multi-kilohertz pulse rates with high beam quality.

1. Introduction

The production of high average power coherent UV radiation is one of the "hot topics" in laser engineering, largely due to the myriad of important applications for short-wavelength radiation. These applications include precision micromachining, photolithography for integrated circuit manufacturing, and fluorescence mapping for medical and industrial diagnostics. While excimer lasers represent the most established technology for generating UV laser radiation, they have some fundamental limitations — principally repetition rate and beam quality — that can limit their applicability. Within the Centre for Lasers and Applications at Macquarie University, we have developed techniques to generate high power UV by nonlinear frequency conversion from high average power, high pulse rate visible sources. Almost all our work has used the pulsed copper vapour laser as the visible laser source, however many of the techniques we have developed could be applied to other sources such as high-repetition-rate frequency-doubled diode-pumped Nd^{3+} lasers.

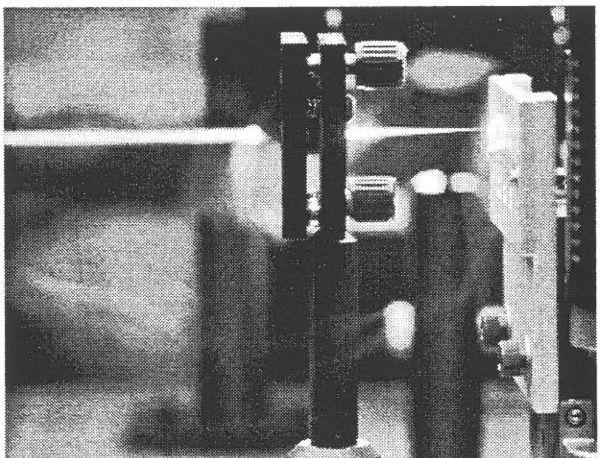

***Figure 1:** Ultraviolet machining using a frequency doubled copper-vapour laser.*

In this article, I review recent work at the Centre for Lasers and Applications on UV generation from copper vapour lasers. After considering the relevent issues of copper laser technology and nonlinear frequency conversion, I discuss the challenges in generating high power UV, and how these challenges are being met. Our most recent progress in UV generation, which has involved power scaling to the 5W level and beyond using enhanced copper vapour lasers, will then be described. Finally, I discuss some of the applications for frequency-doubled copper vapour lasers which include precision micro-machining [1], as shown in Figure 1.

2. Copper Vapour Lasers – Recent Developments and High Beam Quality Generation

Copper vapour lasers (or CVLs) are high average power pulsed gas lasers emitting on the green (510.6 nm) and yellow (578.2 nm) atomic transitions in the copper atom. The green to yellow power ratio is typically about 3:2. Copper vapour lasers are operated at pulse repetition frequencies (PRFs) ranging from 5 kHz to 20 kHz, and produce short output pulses, ranging from about 20 ns to 50 ns duration at base. Commercial CVL devices capable of output powers up to 100W are readily available, and devices producing more than 500W have been reported.

As is typical of gas lasers, power scaling is achieved by scaling the output aperture and active volume. For example, a typical 20W CVL has a 20-25mm diameter output beam and a 1m long active volume, while a 100W CVL has a 60-80mm diameter output beam and a 1.5–2m long active volume. The visible output of CVLs is widely used in a range of industrial and medical applications, which are extensively reviewed in reference [2].

Laser action in copper vapour is achieved by passing a pulsed electrical discharge through a mixture of copper vapour and neon buffer gas. The copper vapour is most commonly generated by evaporation of the elemental metal (the so-called "high temperature CVL"), but can also be obtained by the evaporation and subsequent discharge dissociation of a volatile copper halide compound (usually CuBr). These devices are called copper halide lasers. A recently developed variant of the copper halide laser, where copper bromide is generated *in-situ* by flowing reactive HBr gas over solid copper pieces, is called a copper HyBrID (**Hy**drogen **Br**omide

In Discharge) laser [3]. Apart from the differences in copper production mechanisms, these lasers also exhibit some key differences in their gain behaviour, which has important implications for high beam quality operation of CVLs.

Many potential applications of CVL light, including nonlinear frequency conversion, require high beam quality or low divergence. However, the intrinsic beam quality (or divergence) of CVL output is very poor — typically about 100 times the diffraction limit — leading to their description by many as "big green flashlights". The poor intrinsic beam quality is a result of the very high gain, large gain volume, and short gain duration of these systems [4]. High beam quality output can be obtained from CVLs, however, by using very high magnification (M=50 to 200) unstable resonators. The output beam quality then evolves, in a stepwise fashion down to the diffraction limit, through the output pulse [5].

Not all the raw power of a CVL can be extracted as high beam quality (HBQ) output, however, because of the tight propagation constraints imposed by the unstable resonator. As an example, a 20W-rated conventional CVL will only produce about 10W HBQ output when operated with an M=100 unstable resonator. The efficiency of HBQ extraction depends on the detailed gain behaviour and the physical characteristics (plasma tube aperture and length, speed of excitation circuit) of the particular CVL device. In general, the larger the CVL, the poorer the HBQ extraction — a fact which has limited the power scaling of HBQ output of CVL oscillators in the past, and forced researchers requiring more HBQ power to resort to multi-CVL systems.

Thankfully, it turns out that we have recently developed an "escape clause" that does allow high power and good beam quality to be obtained from a single CVL oscillator. This development has been critical in achieving the UV performance reported later in this article. While researching the effects of trace impurity gases (ie other than copper and neon) on CVL performance, we discovered that some gases can substantially alter the spatial and temporal evolution of gain in the laser, by virtue of subtle changes to the discharge kinetics. Further, we have shown that these gain effects can be exploited to dramatically improve the HBQ extraction from a given CVL oscillator. Our recent work has shown that HBQ power extraction from Cu HyBrID lasers can be very high, due to the strong axial concentration of gain and longer gain duration in these systems [6] — a result of the presence of HBr in the plasma. Our own large-scale Cu HyBrID laser can produce about 70W of HBQ output (green and yellow) at a PRF of 15kHz, which is substantially more HBQ power than can be obtained from *any* conventional high temperature CVL oscillator.

Another exciting development has been a new gas additive technique for high temperature CVL devices, which we call Kinetic Enhancement (ie KE-CVLs). This approach, which uses a halogen donor gas additive, provides dramatic improvements in raw and HBQ power from high temperature CVLs [7]. We have demonstrated that the raw output can be more than doubled by using this gas admix scheme, while the HBQ power can be increased by a factor of 2-3. For example, the 20W-rated conventional CVL mentioned earlier produced up to 50W raw power, and 25W HBQ power with an M=100 unstable resonator, when kinetically enhanced. We have also obtained HBQ powers of 70W from a larger KE-CVL. These two new "flavours" of CVLs, namely the Cu HyBrID laser and the KE-CVL, represent substantially superior HBQ sources than conventional devices for applications such as nonlinear frequency conversion, and work is continuing in our laboratories to develop these system further.

3. Second Harmonic and Sum Frequency Generation

It has long been recognised that efficient nonlinear frequency conversion of CVL output to the UV would provide an attractive UV source of high average power, high PRF, and high beam quality. Second harmonic generation (SHG) and sum frequency generation (SFG) are standard techniques of nonlinear frequency conversion for generating new wavelengths from existing laser sources [8]. The techniques involve passing either a single beam (SHG) or two beams (SFG) through an appropriate nonlinear optical medium. The nonlinear induced polarisation in the medium causes light to be produces at the the second harmonic frequency (SHG) or at the sum frequency (SFG). Because the process relies on the second-order nonlinear terms in the polarisation, which are generally small, the fundamental fields need to have high power in order to obtain good conversion efficiency to the sum frequency/second harmonic field. This is most commonly attained using high peak power pulsed laser sources, or by using cavity resonant enhancement techniques with CW laser sources.

We are able to use SHG for doubling the green and yellow lines to 255 nm and 289 nm respectively, and SFG for producing 271nm light (see Table 1).

UV Wavelength	Interaction
255.3nm	SHG green
271.2nm	SFG (green + yellow)
289.1nm	SHG yellow

Table 1: *UV wavelengths from SHG/SFG of CVLs*

To attain good conversion efficiencies to the second harmonic or sum frequency, there are a number of requirements to meet. This is most readily appreciated by considering the simplest possible "model" case of second-harmonic generation — that is, SHG with a plane-wave input beam in a thin slab of nonlinear optical material. The second harmonic power $P(2\omega)$ generated by fundamental of power $P(\omega)$ and angular frequency ω, in a thin slab of nonlinear material of thickness L and effective nonlinearity d_{eff} is

$$P(2\omega) = \frac{8\mu_0^{3/2}\varepsilon_0^{1/2}\omega^2 . d_{eff}^2 P^2(\omega) L^2}{\pi h^2 . n(2\omega) n^2(\omega)} \left[\frac{\sin(\Delta kL/2)}{\Delta kL/2} \right]^2$$

Here $n(\omega)$ and $n(2\omega)$ are the refractive indices of the nonlinear medium at the fundamental and second harmonic wavelengths, h is the fundamental spot diameter, and Δk is the magnitude of the wave-vector mismatch (ie magnitude of $\Delta\mathbf{k}$) defined as

$$\Delta\mathbf{k} = 2\mathbf{k}_\omega - \mathbf{k}_{2\omega}$$

where $\mathbf{k}_\omega$ and $\mathbf{k}_{2\omega}$ are the wave vectors of the fundamental and second harmonic waves respectively. Note that, as the conversion efficiency goes up, the above expression for $P(2\omega)$ needs to be modified to account for the reduction of fundamental power as it is converted to the second harmonic, an effect which is called *pump depletion*.

The expression for $P(2\omega)$ suggests the following prerequisites for obtaining good conversion efficiency:

(1) Large d_{eff} (ie high nonlinearity);

(2) High irradiance. $I(\omega)=P(\omega)/\pi h^2$ should be as high as possible, but lower than the damage threshold of the material;

(3) Long crystal (or long interaction length) L;

(4) $\Delta k=0$, called the *phase-matching* condition.

The first two points (and how to deal with them to ensure good conversion) are relatively straightforward. For instance, achieving high power densities may require focusing of the input beam (in which case the functional form of the second harmonic power $P(2\omega)$ is slightly different). Choice of optimum crystal length is often more s+ubtle than suggested by this simple model, as the effects of back-conversion (conversion of the second harmonic back to fundamental) under high conversion conditions can place an effective limit on crystal length, as can the phenomenon of walk-off (described later).

The fourth point — the phase matching condition — is equivalent to ensuring that the fundamental and second harmonic waves move through the nonlinear material at the same phase velocity. This is where "the fun begins". The first problem is that Δk cannot generally be made zero in an isotropic material with normal dispersion, since $n(2\omega)>n(\omega)$. The solution to this problem is to use birefringent materials, and propagate one beam as an ordinary or, o-wave, and the other as an extraordinary, or e-wave, choosing the angle of propagation relative to the crystal axes so that $n(2\omega) = n(\omega)$. If we restrict ourselves to considering one class of birefringent materials, negative uniaxial materials, then there are two possible interactions. The first, called a Type I interaction, propagates the fundamental waves as o-waves and the second harmonic as an e-wave (also known as an *ooe* interaction). The second, called a Type II interaction, propagates the fundamental as o-waves and e-waves (ie polarised at 45^0), while the second harmonic propagates as an e-wave (this is also known as an *eoe* interaction). In general, to achieve the phase matching condition, the angle of propagation relative to the optic axis needs to be adjusted to provide the correct effective refractive indices for the e-waves. This is called *critical* or *angle-tuned phase matching*. There are other forms of phase matching that can be used, however for UV generation from CVLs only critical phase matching is currently a viable option.

Even when critical phase matching can be achieved, the requirement for $\Delta k=0$ places restrictions on the divergence of the fundamental beam, leading to a criterion for the *acceptance angle* of the nonlinear crystal. Equivalently, the temperature dependence of the refractive indices in these media also leads to a *temperature bandwidth* condition as well. Another related issue in critical phase matching is that the Poynting vector of the second harmonic is not parallel to the direction of propagation. This leads to the phenomenon of *walk-off,* where the second harmonic power migrates away from the fundamental beam. All of these issues can restrict the conversion efficiency, if care is not taken in the design of the nonlinear frequency conversion scheme.

4. UV Nonlinear Materials

A significant challenge that has slowed the development of effective UV sources based on SFG/SHG of visible laser radiation has been the paucity of good nonlinear materials. Even now, there are relatively few materials that are suitable for high average power SHG/SFG into the UV — most suffer from either poor transparency, phase-matching capability, or damage threshold. Currently, the best nonlinear materials for CVL frequency doubling applications are the borates (beta-barium borate or BBO, and caesium lithium borate or CLBO). These materials are relatively new — BBO was only discovered about 12 years ago, and only became commercially available about 10 years ago, while CLBO was only discovered about 2 years ago. The relevant parameters of these materials for SHG of green CVL output are given in Table 2.

	BBO	CLBO
Interaction	Type I	Type I
Phase-match angle	$\theta = 50.6^\circ$	$\theta = 68^\circ$,
	$\phi = 0^\circ$	$\phi = 45^\circ$
Nonlinearity (d_{eff})	1.7pm/V	0.9pm/V
Walk off	4.7^0	1.6^0
Acceptance Angle	0.2 mrad.cm	0.5 mrad.cm
Temperature Bandwidth	4^0C.cm	

***Table 2:** Important parameters of BBO and CLBO for SHG of CVL green output.*

BBO is a highly birefringent material, with very narrow acceptance angle and large walk-off angle. CLBO has smaller birefringence, and hence less walk-off and wider acceptance angle, although it has a smaller nonlinearity than BBO. BBO has a small temperature bandwidth (~4°C.cm), which is an issue because BBO has a small amount of residual absorption in the UV (several %/cm), which can lead to self heating and subsequent thermal detuning when generating high average power UV.

5. Challenges and Solutions in CVL SHG/SFG

Having reviewed the relevant issues in CVL technology, second harmonic generation, and UV-capable nonlinear-optical materials, we are now in a position to discuss why efficient SHG of CVL output is not as straightforward as "putting a crystal in the beam". The first challenge is that CVLs are only a moderate peak power source (10-200kW) which, in combination with their large beam size, means they are inherently restricted in their peak unfocused irradiance ($I < 1MW/cm^2$). As a consequence, CVL output needs to be focused into the nonlinear material in order to provide sufficient peak power density (ie $>20MW/cm^2$) to provide good conversion efficiency to the UV. Focussing the pump beam(s) introduces a host of complexities into frequency conversion. Issues such as aberrations in the optical system (which limit conversion efficiency by reducing irradiance and introducing dephasing), the acceptance angle of the nonlinear material when employing critical phase-matching, and walk-off of the UV from the pump field(s) need to be addressed. A related requirement is that the pump beam quality must generally be very high for efficient conversion in critically phase-matched interactions, in order to allow tight focussing, and also to match the narrow angular acceptance of these UV-capable nonlinear materials. Finally, because these UV-capable materials exhibit some residual UV absorption (which increases with proximity to the band-edge) crystal heating and hence thermal dephasing [9] can be a problem when generating high UV powers. This is because pump beam intensity profiles are non-uniform, and so UV generation and subsequent thermal dephasing is non-uniform across the pump wavefront, leading to reduced conversion efficiency.

Early (up to 1992) empirical studies of CVL SHG both in our laboratory and elsewhere (see the review in reference [10]) demonstrated that these challenges were not easy to overcome. While UV output powers up to 0.46W were generated, conversion efficiencies were typically low (<10%), and crystal damage was an enduring difficulty. In these early studies, very high f-number spherical focusing was employed, in order to deliver the maximum fundamental power within the narrow acceptance angle of BBO. However, frequency conversion with long narrow beam waists suffers severely from walk-off effects, which reduces the interaction length and degrades the UV beam profiles. The problem of crystal damage was related to the large changes in power density at the crystal induced by the combination of temporally evolving CVL beam quality and the spherical focusing arrangement.

A major step to circumventing these problems with optical delivery was developed by Coutts and Piper [11] in 1992. They showed that by producing a *line focus* within the nonlinear material, where the beam is collimated in the angle-tuning plane (~3-4mm wide) and focused in the orthogonal direction, UV power generation from a CVL source was dramatically improved — from about 0.5W to 1.3W.

The improved performance of the line focus geometry is a result of several factors. First, the maximum fundamental power propagates within the acceptance angle of the nonlinear medium (since the beam is collimated in that plane). Focusing in the orthogonal direction brings the peak irradiance in the regime where efficient nonlinear conversion takes place, and indeed subsequent studies have shown that optimal focusing in this plane is quite tight (~f/16) [12]. Another advantage is that the temporally evolving CVL beam quality does not induce such large changes in power density at the crystal, since focusing is in one plane only, which substantially reduces problems with crystal damage. The line focus also minimises problems with walk-off, since walk-off is in the plane of the line focus where the fundamental beam is wide. Finally, problems with thermal dephasing are reduced, since heat generation is spread across the crystal.

By using a slightly improved line focus system, output power from a single CVL oscillator was subsequently scaled to 1.75W [12], while output power up to 3.6W at 255nm (SHG Green) was generated using a CVL master-oscillator power amplifier system. In the former case, instantaneous conversion efficiencies up to 50% were observed, while the average conversion efficiency (green fundamental power to UV power) was ~35%.

6. Recent UV Power Scaling Experiments

As I noted earlier in Section 2, one of the fundamental restrictions on UV power scaling with CVLs is obtaining sufficient HBQ output powers. Recently, our development of kinetically enhanced CVLs has dramatically expanded the HBQ power capability of single CVL oscillators, and we have investigated the UV generation capability of a KE-CVL device. The particular KE-CVL we used is the one described earlier, which produces ~25W total (green + yellow) HBQ output at 10kHz PRF. At the nonlinear crystal, 13.5W of HBQ green was available for SHG.

The optical configuration used to produce the line focus for SHG of the KE-CVL output is shown in Figure 2. The KE-CVL was operated with an unstable resonator of magnification M=100, incorporating a 4m radius of curvature (R) high-reflecting mirror and an R = –40mm convex reflector (see figure 1). An intracavity polarising beam splitter ensured linearly polarised output. A mirror telescope, consisting of an R = 2m concave primary mirror and a concave re-collimating mirror with ROC of 25cm compressed the 25mm KE-CVL output beam to 3.2mm diameter. Once compressed, the pump beam was focused into the nonlinear crystal using a cylindrical lens of focal length f=38mm. Both nonlinear crystals (BBO and CLBO) were $6\times4\times10mm^3$ in size.

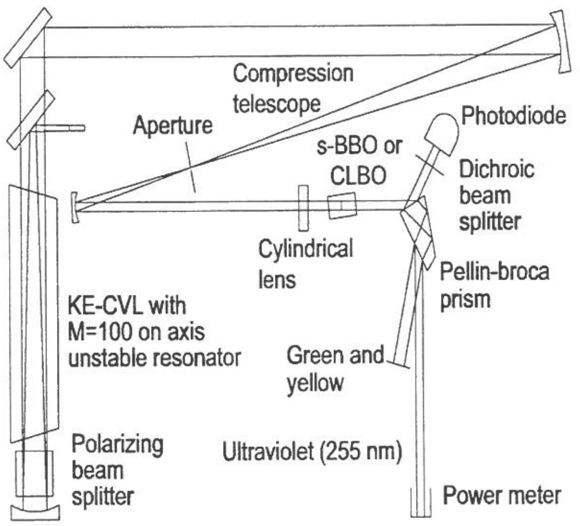

Figure 2: Optical arrangement used for SHG of KE-CVL output.

Table 3 summarises the performance of SHG of the KE-CVL output. The UV powers are corrected for prism losses (7%), but do not account for reflection losses at the nonlinear crystal.

Nonlinear Material	Fundamental Average Power	UV Average Power	Wallplug Efficiency
CLBO	13.5 W	**4.7 W**	0.12%
BBO	13.5 W	**3.9 W**	0.1%

Table 3: *UV Generation using a kinetically enhanced CVL.*

A maximum of 4.7W UV power (at 255nm) was generated from the KE-CVL when using CLBO as the nonlinear material, with average conversion efficiency of 35% and wall plug efficiency of 0.12%. For the same fundamental power, SHG using BBO produced slightly less power (3.9W). These UV powers are up to 2.7 times higher than previously observed for SHG of the output from a single CVL oscillator, and the wallplug efficiency is up to 2.4 times higher.

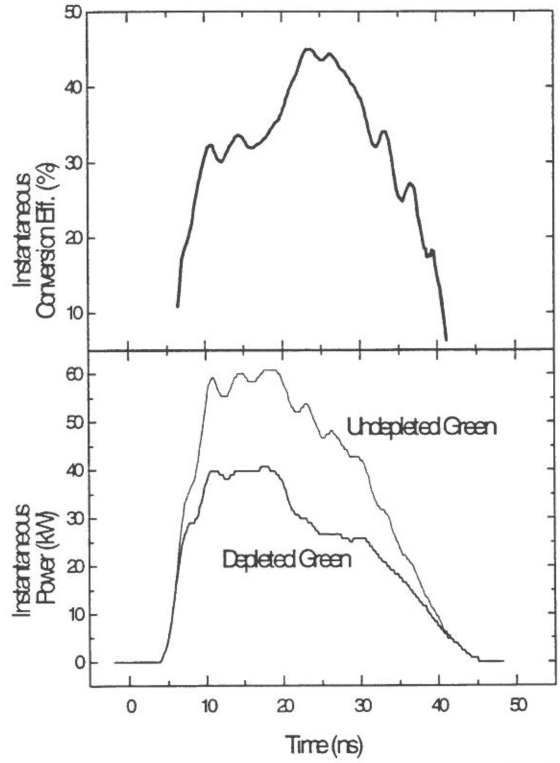

Figure 3: Green (fundamental) pulse shape from KE-CVL, without conversion to UV (undepleted) and with conversion to UV (depleted), when using BBO as the nonlinear material. The instantaneous conversion efficiency derived from the fundamental depletion is also shown.

Figure 3 shows a comparison between the fundamental pulse shape when the BBO was oriented for phase matching (ie depleted fundamental) and when the BBO was oriented away from phase matching (undepleted fundamental). Also shown is the instantaneous conversion efficiency of visible to UV, determined from these pulse shapes. What is most interesting to note is the "jump" in conversion efficiency about half-way through the fundamental pulse. We know from other measurements that this "jump" coincides with the *stepwise* improvement of the beam quality of the fundamental input beam at this time. When CLBO is used as the nonlinear material, however, the pulse shape and temporal conversion efficiency data (not shown) does not exhibit as dramatic a jump in conversion efficiency at this time.

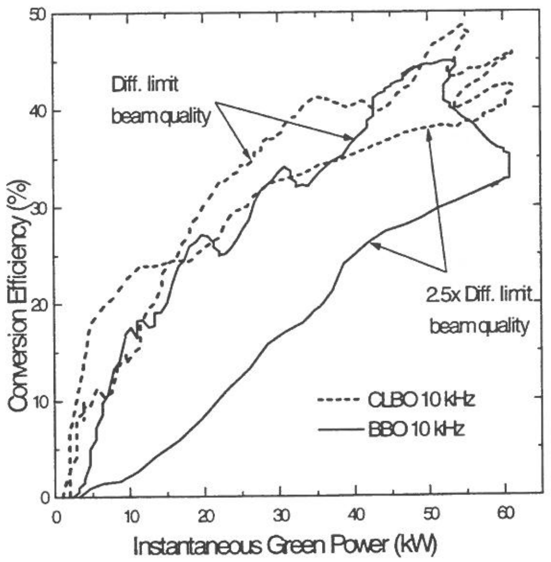

Figure 4: Conversion efficiency of KE-CVL output to UV, as a function of instantaneous green power, when using CLBO and BBO.

The effect of the temporal evolution of CVL beam quality on SHG efficiency is also evident in Figure 4. This figure shows variation of conversion efficiency with instantaneous fundamental power, as derived from the fundamental pulse shapes. For BBO, there is a clear difference (~15%) between the instantaneous conversion efficiency for first half of the pulse, which has poorer beam quality (around 2-3 times diffraction-limited) than the latter half of the pulse (which has essentially diffraction-limited beam quality). For CLBO however, the instantaneous conversion efficiency does not vary as markedly between these divergence components. This demonstrates that the larger acceptance angle of CLBO enables higher conversion efficiency of the poorer beam quality component than in BBO, despite the lower nonlinearity of this material. In addition, the conversion efficiency for *each* divergence component in CLBO is higher than in BBO, which suggests that the reduced UV walkoff in CLBO and/or lower thermal dephasing due to the better UV transmission of CLBO assist in providing higher overall conversion efficiency.

We found that our CLBO sample was not as robust as BBO. Within a day or two of using the crystal for the first time, we found that it stopped producing UV. It has subsequently been learned that CLBO is extremely susceptible to damage relating to the absorption of trace amounts of atmospheric moisture, which distorts the refractive indices of the material [13]. There is continuing work being undertaken to address this problem, with approaches such as housing CLBO in a sealed cell, maintaining it at elevated temperature (~150^{0}C) at all times, or Al doping of the crystal, being trialled to eliminate this problem.

Another point to note is that the conversion efficiency to the UV observed at these fundamental power levels is essentially the same as observed by Coutts [12] at much lower fundamental power (~5W). This insensitivity to fundamental power scaling demonstrates the good thermal management provided by line focusing.

7. Beyond 5W UV

Following the successful scaling of UV power using a KE-CVL source, we recently performed a short trial of UV generation using our newly completed large-scale Cu HyBrID laser. This device produced up to 70W of HBQ output (~40W green) at 15kHz PRF, which represents another large step in fundamental average power capability for nonlinear frequency conversion.

A similar arrangement as used for the earlier work on SHG of KE-CVL output (shown in figure 2) was employed for this experiment. The green output of the Cu HyBrID laser was separated from the yellow using a dichroic mirror. This beam (~30mm diameter) was compressed to 4mm diameter using an R=1.5m/R=0.2m mirror telescope, and then focused into BBO (6×4×10mm^3 crystal) with an f=38mm cylindrical lens.

From the 40W green fundamental, we obtained a maximum UV power of 7.85W at 255nm (SHG green). This represents the highest UV power ever obtained from a single CVL oscillator of any type. However, the average conversion efficiency in this case (~20%) was substantially lower than we have been obtaining at lower fundamental powers. While optimising the UV output in this case, it was clear that thermal dephasing was interfering with UV generation, and there was evidence that other deleterious thermally-induced effects (such as birefringence) were also playing a role in limiting the conversion efficiency. By addressing the issue of thermal dephasing through thermal and optical design, we hope that conversion efficiency can be maintained at the high fundamental power level now available, to provide UV sources with more than 10W of power.

8. Applications of UV from CVLs

One of the prime applications for UV-CVLs (ie CVLs with SHG stage) is in micromachining, particularly of polymeric substances. The strong absorption of UV in most polymers provides clean, controllable ablation, allowing the precise machining of very small structures. An example is shown in Figure 5, which shows a 70μm diameter hole drilled in polyethylene film. A fuller description of micro-machining using UV-CVLs can be found in an earlier edition of *AOS News* [1].

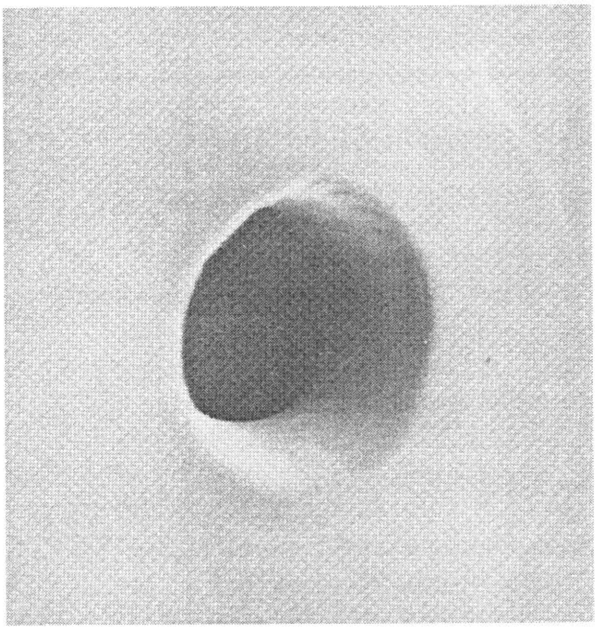

Figure 5: Scanning electron micrograph of a 70 μm hole drilled in polyethylene using a frequency-doubled CVL.

Another recently developed UV-CVL application is high spatial resolution microanalysis of rock samples. In this application, UV-CVL is used to ablate microscopic volumes of rock for mass spectrometric analysis, to determine oxygen isotope ratios of silicate and oxide minerals [14]. The high beam quality of the UV and the high PRF are both important for providing the fast sample analysis and high spatial resolution required for this application.

Finally, another "application" we are currently pursuing is the use of the UV-CVL as a source for nonlinear frequency conversion deeper into the ultraviolet. Such deep UV is highly desirable for such applications as photolithography, opthalmology, and micro-machining of high band-gap materials. In a pilot experiment, we have demonstrated that deep UV radiation can be generated by SFG of the UV output from a frequency-doubled CVL system with the IR output of a diode-pumped Nd:YLF laser system, to produce output at 205nm. Using this scheme, we have generated output powers (at 205nm) of more than 0.25W from the output of a standard UV-CVL (1.5W 255nm) and a Spectra-Physics TFR diode-pumped Nd:YLF laser (0.95W) at a PRF of 5kHz. In the future, we plan to investigate power scaling in the deep UV by using our recently developed UV sources and a more powerful diode-pumped Nd^{3+} laser.

Acknowledgments

Work in the nonlinear frequency conversion of CVLs within the CLA has been very much a team effort. I would like to acknowledge the researchers who have made significant contributions to the work described in this article: Dr David Coutts (now at Oxford University), Mr Rodney Trickett, Dr Michael Withford, Dr Richard Mildren, Ms Elizabeth Illy, Dr Robert Carman, and Dr David Jones (of Heriot-Watt University). Thanks also to Dr Ben Duval, of BHP CRL, for the loan of the Spectra Physics TFR diode-pumped Nd:YLF laser for the deep UV experiments. Finally, I also acknowledge the substantial contribution of Prof J. A. Piper, who provided the impetus for this work, and for his many useful and important discussions throughout its duration.

References

1. E K Illy, A C J Glover, J A Piper, "Ultraviolet Laser Micromachining," *AOS News* **10**(4) (1996) 21-23.
2. C E Little, N V Sabotinov (eds) "Pulse Metal Vapour Lasers," Dordrecht: Kluwer (1996).
3. D. R. Jones, A. Maitland, and C. E. Little, "A high-efficiency 200W average power copper HyBrID laser," *IEEE J. Quantum Electron.* **QE-30** (1994) 2385-2390.
4. D. W. Coutts and D. J. W. Brown, "Formation of output in copper vapour lasers," *Applied Optics* **34** (1995) 1502-1512.
5. D. W. Coutts, "Time resolved beam divergence from a copper vapour laser with unstable resonator," *IEEE J. Quantum Electron* **QE-31** (1995) 330-342.
6. D J W Brown, C G Whyte, D R Jones, C E Little, "High-beam quality, high-power copper HyBrID laser injection-seeded oscillator system," *Opt. Commun.* **137** (1997) 158-164.
7. M J Withford, D J W Brown, R J Carman, J A Piper, "Kinetic enhancement of copper vapour lasers using halogen donor gas additives," Tech. Dig IQEC '96, Opt. Soc. Amer. (1996) paper ThQ8.
8. Y R Shen, "The Principles of Nonlinear Optics," New York: John Wiley and Sons (1984).
9. D T Hon, in *Laser Handbook*, M L Stitch, Ed. Amsterdam: North Holland, 1979
10. D W Coutts, D J W Brown, "Production of High Average Power UV by Second-Harmonic and Sum-Frequency Generation from Copper-Vapor Lasers," *IEEE J Sel. Topics Quantum Electron.* **1** (1995) 768-778.
11. D. W. Coutts and J. A. Piper, "One watt average power by second harmonic and sum-frequency generation from a single medium-scale copper vapour laser," *IEEE J. Quantum Electron.* **QE-28** (1992) 1761-1764
12. D. W. Coutts, "Optimisation of line focusing geometry for efficient nonlinear frequency conversion from copper vapour lasers," *IEEE J. Quantum Electron.* **QE-31** (1995) 2208-2214
13. Y K Yap, Y Mori, S Haramura, A Taguchi, K Nishijima, T Inoue, A Miyamoto, H Sasaki, Y Kagebayashi, T Sasaki, "Stable operation of CLBO crystal for laser frequency conversion at elevated temperature," Tech. Dig. CLEO '97, Opt. Soc. Amer. (1997) paper CFM4.
14. E. D. Young, A. J. Andrews, D. W. Coutts, "Oxygen isotope ratio analysis of silicate and oxide minerals by UV ablation with a frequency doubled copper vapour laser," CLEO/Europe (1996) paper CWF71.

NEW from **WARSASH Scientific**

P-517.2C, P-527.2C XY Piezo Flexure Frame from PI

- **Travel range 100 x 100 & 200 x 200 µm**
- **Fast settling time**
- **Integrated capacitive displacement sensors**

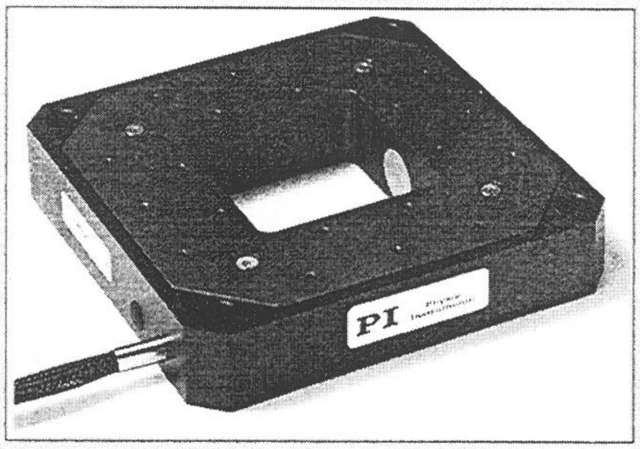

P517 and P-527 are fast, high resolution, piezoelectrically driven XY flexure stages. They provide a travel range of 100 x 100 and 200 x 200 µm, respectively and a clear aperture of 66 x 66 mm. The stages are ideally suited for optical applications such as confocal microscopy, near-field scanning microscopy or mask alignment.

Working principle: Low voltage PZTs (0 to 100 V) and flexures are employed as the drive and guiding system. The flexures provide for zero-backlash motion and excellent guiding accuracy. Integrated capacitive displacement sensors measure the position of the moving frame providing possible resolution on the order of 1nm.

Application examples: Micropositioning, scanning microscopy, optics, laser-technology, micro-manufacturing.

OXFORD LASERS

New Fibre Light Sheet Device

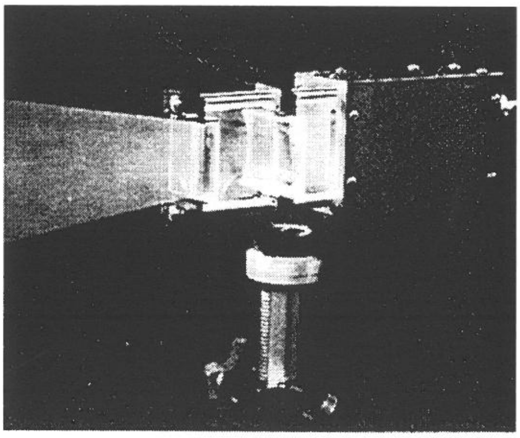

One of Oxford Lasers' latest developments is a unique device which enables laser light to be delivered by high power transmission optical fibre direct to the point of interest.

The Fibre Light Sheet is a truly innovative concept which breaks through the divergence barrier, allowing light sheets to be generated where required and effectively de-couples the laser from the point of interest.

WARSASH Scientific tel: (02) 9319 0122 - fax: (02) 9318 2192
email: warsash@ozemail.com.au - http://www.ozemail.com.au/~warsash

LASTEK

....making light work!

LASERS -	Spectra-Physics Lasers Opto Power Corp Schwartz Electro Optics Omnichrome Aerotech Lexel
LIGHT SOURCES -	Oriel Instruments
SPECTROMETERS/MONOCHROMATERS -	Oriel Instruments
OPTICAL DETECTION SYSTEMS -	Oriel Instruments
CCD CAMERAS -	Photometrics Oriel Instruments
OPTICAL MOUNTS -	Aerotech Oriel Instruments New Focus ThorLabs
OPTICAL TABLES -	TMC CleanTop™
MINIATURE SPECTROMETERS -	Ocean Optics
ELECTRO OPTICS/ACOUSTO OPTICS -	Conoptics Cleveland Crystals Isomet
LASER OPTICS -	CVI Spectra-Physics
DETECTORS -	UDT Sensors Silicon photodiodes Sensors Unlimited In Ga As Photodiodes
GENERAL OPTICS -	Oriel Instruments CVI Edmund Scientific
LASTEK PRODUCTS -	Software for spectroscopy Custom power supplies Custom systems and consulting
FIBRE OPTICS -	Spectran Specialty Fibre Oriel Instruments
LASER POWER METERS-	Spectra-Physics Lasers Scientech

LASTEK Pty Ltd - Head Office: Thebarton Campus, 10 Reid St, Thebarton, SA 5031
Adelaide HQ tel: (08) 438 668 fax (08) 438 427 e-mail: lastek@www.saschools.edu.au

PHOTON ENGINEERING

NEW

FAST ACCURATE LASER BEAM PROFILING MADE EASY

With *BeamPro* from Photon Inc.

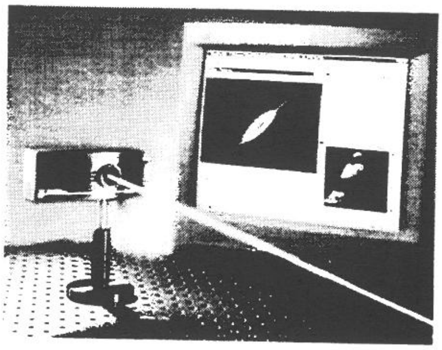

With a host of features *BeamPro* provides the ultimate in flexibility and ease of use with a quantum leap in laser beam profiling technology:

- Built-in variable attenuator for safe use over a wide incident power range for pulsed or CW beams.
- Plug-in PC card for flexibility in any R & D, QA, or process control setting.
- Slim-line head allows placement inside optical systems.
- Measure beamwidths down to 95 μm. Better than any camera based product previously available.
- Powerful MS-Windows based software provides a huge range of analysis and control tools.

TUNABLE PULSED ALEXANDRITE LASERS

From Light Age, Inc

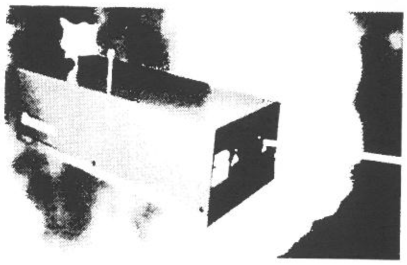

Features of Alexandrite lasers:

- Tunable over 720-800 nm.
- 200-2400 nm range with frequency conversion options.
- 10-300 mJ pulses over entire UV / VIS / IR range.
- 100 ps - 2 μs pulse widths available.
- Flashlamp pumped or diode laser injection seeded.

Also Available: CW UV laser nUVo with 5 - 10 mW output at 360 - 400 nm

GET INSIDE THE CAVITY

with the new Lightbook LAB from Light Solutions

Introducing the innovative Lightbook & Lightbook LAB from Light Solutions Corp providing over 10 W TEM_{00} of 1064 nm output from diode-pumped $Nd:YVO_4$ and Nd:YAG laser systems.

Features include:

- CW or Q-Switched from 1 kHz to 100 kHz.
- LAB version has hermetically sealed laser head with external output coupler and mount allowing direct access to inside the cavity. With this versatile design, intracavity experiments (e.g. doubling / quadrupling or OPO) can be performed on an optical bench while retaining the benefits of a hermetically sealed commercial laser head.

PHOTON ENGINEERING
Postal: PO Box 10269, Gouger St
Shipping: 1st Floor, 123 Wright St
Adelaide, South Australia, 5000

Tel (08) 8410 4599
Fax (08) 8410 4544

IQEC '96: General Chair's Report

Introduction
The XX International Quantum Electronics Conference was held at the Sydney Convention and Exhibition Centre, Darling Harbour, Sydney, Australia 14-19 July, 1996. This was the first time that the Conference had been held in the Southern Hemisphere, and of course it was independent of CLEO/QELS which was held in Anaheim in June. Euro-CLEO was held some 2 months later, in September. Although there was some anxiety that the other two meetings would detract from the attendance at IQEC '96, there was evidence that the three meetings were quite strongly differentiated by the international QE community. IQEC '96 subsumed the biennial Australasian Conference on Optics, Lasers and Spectroscopy (ACOLS) and as such provided an outstanding opportunity to Australian and New Zealand scientists working in this area to present their work to and interact with an international audience. The General Organising Committee was delighted that so many of our colleagues took this opportunity and in so doing gave their strong support to the conference. Feedback at the conference and subsequently has confirmed the view that the quality of the papers presented at IQEC '96 was at the highest international standard. We have also been congratulated (by the OSA, no less) for the overall standard of the organisation and physical facilities and arrangements. In general I think that we can be pleased that IQEC '96 has given a significant boost to QE research undertaken in our region.

Organisation
The General Organising Committee worked effectively, and was strongly supported by the ACQE and the local QE community in general. Chris Walsh as Finance Chair, Ken Baldwin as Exhibition Chair, John Harvey as Publicity Chair and Brian Orr as Functions Chair and ACQE Liason did outstanding jobs. We also received strong support at critical times from Dan Walls and Wes Sandle, and special mentions are due to Hiroshi Takuma, Peter Knight and Tom McIlrath, who helped us with ticklish international issues. Our experiences with the local professional conference organisers were mixed: we certainly had to exercise very tight control over spending and there were problems with their administrative systems, but they performed well on-site.The Sydney Convention and Exhibition Centre was generally well-suited to a meeting of this size and we had very favourable responses from international visitors to the standard and location of the facility. One trap was the extremely high cost of audio-visual and related services at the Centre which caused a serious rise in the ChairÕs blood-pressure at the eleventh hour. The weather was superb, of course. There being almost zero negative comment, there seems to have been a high level of satisfaction with the conference accommodation. Over 200 attendees chose the low-cost accommodation in student halls; this we expected since there was a high attendance from interstate Australia and NZ, but quite a large number of international attendees also chose this option.

Technical Program
The Technical Program Committee operated very effectively under the outstanding leadership of Juergen Mlynek. Peter Hannaford, Gerard Milburn and the other Subcommittee Chairs did excellent work, and were ably assisted by many of our colleagues as Subcommittee members. It was necessary that the General Chair maintain very close liason with the TPC in the context of a meeting of this type. The decision to use OSA Conference Services to handle incoming papers to the selection stage proved to be a very good one. Naomi ChavezÕ team were outstanding in every way and their assistance up to and including the Program Committee Meeting in San Jose was invaluable, and reasonably priced.

An analysis of papers delivered at the conference by category and region/country of origin is given in Attachment 1. There were 637 papers submitted, of which 472 were accepted as regular papers and 20 upgraded to Invited Papers representing an overall acceptance rate of 77%. The TPC was satisfied that the standard of the accepted papers was comparable to that of previous meetings. The number of submissions was above that expected, but this was accommodated using expanded poster sessions. There were 36 Postdeadline submissions, of which 14 were chosen for oral presentation (38%); a further 16 were chosen for presentation in a Postdeadline Poster session, which received quite favourable comment.

Registrations
A summary of registrations is given in Attachment 2. The final number of 666 was comfortably above the low-end target of 600 and somewhat below our high-end target of 800. Registrations from Australia/NZ were above target, as were those from Europe. Registrations from Japan, China and SE Asia were somewhat below target and from North America rather disappointing (CLEO/QELS may have been a factor in the latter). Student registrations were excellent, approximately one third of these coming from outside Australia.

Finance

A summary statement of Income and Expenditure for IQEC '96 is given in Attachment 3. Note the Conference and Exhibition operated as separate cost centres. The Conference operated very close to budget throughout and in the event finished with a small surplus of $5,000. Revenue for the Exhibition was below target despite some very hard work by the Exhibition Chair, Ken Baldwin. In fact we succeeded in getting every QE-related company operating in Australia to exhibit but only 4 companies from outside Australia. Though the Exhibition was very small by US standards, it was significant on the local scale and we had very positive feedback from the exhibitors, as well as the conference attendees, who enjoyed the time to speak to suppliers at leisure and in detail. However the low revenue and fixed costs resulted in a loss for the Exhibition of $5000 and an overall outcome of almost exact break-even.

The costs of IQEC '96 were strongly underpinned by a total of $180,000 in unsecured loans from various sources: The Australian Optical Society ($15.000), The Institution of Engineers (Australia)($15,000), Macquarie University ($125,000) and The Commonwealth Special Research Centre for Lasers and Applications ($25,000). Each of these loans has been repaid in full. Substantial cash grants were received from several organisations, notably IUPAP ($20,000), The Australian Photonics Cooperative Research Centre ($10,000), The Commonwealth Special Research Centre for Lasers and Applications ($10,000) and The BHP Co ($10,000), and valuable sponsorship from Coherent Scientific Pty and Coherent Inc, Spectra-Physics and Lastek Pty, and Applied Laser Technology Pty Ltd.

Final thanks

In addition to those named above I would like to thank the many people who willingly gave their help at times of crisis (and there were plenty of these!): Linda Harris and secretarial staff in my School at Macquarie University (at one stage all 8 were simultaneously keyboarding the last papers for the Digest), David Baer and John Tocher of the CLA who looked after a variety of physical arrangements at the Convention Centre, Danny Brown who did all the signage, and many of my colleagues and graduate students who cheerfully did envelope stuffing and other tedious tasks when called upon. Thanks all!

Jim Piper
General Chair IQEC '96

IQEC '96 Papers by region and country (Attachment 1)

Australasia	**157**
Australia	137
New Zealand	20
Western Europe	**203**
Austria	8
Denmark	8
Finland	1
France	19
Germany	93
Italy	17
Netherlands	2
Portugal	1
Spain	6
Sweden	1
Switzerland	5
United Kingdom	42
Eastern Europe	**27**
Belorussia	1
Estonia	1
Israel	5
Lithuania	2
Russia	15
Ukraine	3
Asia	**93**
Hong Kong	3
India	1
Japan	51
Korea	7
PR China	21
RO China	6
Saudi Arabia	2
Singapore	2
Africa	**1**
South Africa	1
North America	**114**
Canada	6
Mexico	3
USA	105
South America	**5**
Brazil	5
Total	**600**

IQEC '96 Papers by category

Plenary	3
Tutorial	5
Invited	70
Invited (upgraded)	20
Contributed	472
Oral	233
Poster	239
Postdeadline	30
Oral	16
Poster	14
Total	**600**

IQEC '96 Registration by region and country (Attachment 2)

Australasia	**310**
Australia	277
New Zealand	33
Western Europe	**157**
Austria	9
Denmark	5
Finland	1
France	15
Germany	66
Italy	11
Netherlands	2
Portugal	1
Spain	7
Sweden	3
Switzerland	5
United Kingdom	32
Eastern Europe	**11**
Israel	1
Lithuania	1
Russia	8
Ukraine	1
Asia	**89**
Hong Kong	4
India	1
Japan	55
Korea	11
PR China	9
RO China	7
Saudi Arabia	1
Singapore	1
Africa	**1**
South Africa	1
North America	**95**
Canada	5
Mexico	1
USA	89
South America	**3**
Brazil	2
Chile	1
Total	**666**

IQEC '96 Registrations by category

Regular	**460**
Early	345
On-site	115
Student	**203**
Early	158
On-site	45
Day	**3**
Total	**666**

IQEC '96 Conference income and expenditure statement (Attachment 3)

Revenue		**A$000**
Registrations		235
Additional reception inc.		7
Grants:	Australian Govt	8
	IUPAP	20
Sponsorship:	CLA	10
	CRC Photonics	10
	Companies	20
Commissions		17
Sales		4
Total revenue		**321**

Expenditure		**A$000**
Venue hire		34
Audio-visual		11
Display boards and registn booths		7
Functions:	am/pm refresh	13
	Conf receptn	20
	VIP function	13
	Postdeadline fn	4
	Misc functions	5
Production:	Prelim announc	4
	First call	5
	Final call	11
	Adv Program	15
	Tech Digest	31
	OSA Conf Services	17
Attendee support		29
Administration:	PCO	71
	Insurance & banking	10
	Badges and satchels	4
	Stationery & sundries	13
Total expenditure		**316**

IQEC '96 Exhibition income and expenditure

Revenue	**A$000**
Registrations	50
Miscellaneous inc.	1
Total revenue	**51**

Expenditure	**A$000**
Venue hire and services	33
Shell hire	7
PCO	10
Promotion	6
Total expenditure	**56**

IQEC '96 total revenue	372
IQEC '96 total expenditure	372

SPIE and Working Group Membership Application

SEND THIS FORM TO:
P.O. Box 10 • Bellingham, Washington 98227-0010 USA • Phone: 360/676-3290 (Pacific Time) • Telefax: 360/647-1445
E-mail: spie@spie.org • Telnet FTP: spie.org • World Wide Web URL: http: //www.spie.org/

(Please print or type)

↓ Prefix ↓	↓ Last Name ↓	↓ First Name/Middle Name or Initial ↓	↓ Suffix ↓

Title or Position ____________ Company Name ____________

Company Address/Dept./Mail Stop ____________

____

City ________ State ________ Country ________ Zip or Postal Code ________

Business Phone (______) ________ Ext. ________ Telefax ________ Telex ________

E-mail Address/Network ________ Date of Birth ________ ❑ Male ❑ Female

Home Address ____________

City/State/Country/Postal Code ____________

ANNUAL MEMBERSHIP DUES
(check one amount)

SPIE WORKING GROUP DUES	Regular Fellow N. America	Regular/ Fellow Elsewhere	Retired	Student	Student No Journal
Membership with one journal	❑ $ 85	❑ $ 95	❑ $ 25	❑ $ 30	
Membership with two journals	❑ $125	❑ $135	❑ $ 65	❑ $ 70	
Membership with three journals	❑ $165	❑ $175	❑ $105	❑ $110	
Student with no journal	–	–	–	–	❑ $15

Select Journal(s)
❑ *Optical Engineering*, monthly (default)
❑ *Journal of Biomedical Optics*, quarterly
❑ *Journal of Electronic Imaging*, quarterly

Air Shipping Option

For members outside North America, additional charges for **Optional International Surface Airlift** shipping:

❑ *Optical Engineering*	$60
❑ *Journal of Biomedical Optics*	$20
❑ *Journal of Electronic Imaging*	$20

I hereby apply for membership in SPIE, and if elected will be governed by SPIE's Bylaws, Statements of Policies, and Procedures.

Full Signature ____________ Date ________

SPIE WORKING GROUP DUES	SPIE Member	Non-member	
Adaptive Optics	❑ $15	❑ $30	$ ____
BACUS (Photomask Technology)	❑ $25	❑ $50	$ ____
Biomedical Optics Society	❑ $15	❑ $30	$ ____
Electronic Imaging (Cosponsored by IS&T)	❑ $15	❑ $30	$ ____
Fiber Optics	❑ $15	❑ $30	$ ____
High Speed Photography, Videography, and Photonics	❑ $15	❑ $30	$ ____
Holography	❑ $15	❑ $30	$ ____
Laser Communications	❑ $15	❑ $30	$ ____
Lens Design	❑ $15	❑ $30	$ ____
Noninvasive Inspection Technologies	❑ $15	❑ $30	$ ____
Optical Processing and Computing	❑ $15	❑ $30	$ ____
Optical Materials	❑ $15	❑ $30	$ ____
Optomechanical and Precision Instrument Design	❑ $15	❑ $30	$ ____
Penetrating Radiation	❑ $15	❑ $30	$ ____
Photolithography	❑ $15	❑ $30	$ ____
Robotics and Machine Perception	❑ $15	❑ $30	$ ____
Smart Structures and Materials	❑ $15	❑ $30	$ ____
Thermosense (Thermal Infrared Sensing for Diagnostics and Control)	❑ $15	❑ $30	$ ____
X-Ray/UV Optics	❑ $15	❑ $30	$ ____
Health Care Engineering and Technology Policy	❑ $15	❑ $30	$ ____

TOTAL PAYMENT AMOUNT$ ________
METHOD OF PAYMENT
❑ **Check enclosed (write applicant's name on check).**
Make payable to SPIE. Mail to SPIE, P.O. Box 10, Bellingham, WA 98227-0010 USA.
(Payment in U.S. dollars—by draft on a U.S. bank, or international money order—is required. Do not send currency.
If payment is made by bank transfer include copy of the transfer order.)

Charge to my: ❑ **VISA** ❑ **MasterCard**
❑ **American Express** ❑ **Diners Club**

Account Number (Please list all digits from your charge card)

____

Expiration Date ____________

Signature ____________
required if using charge card

FOR OFFICE USE ONLY
Date ________
Amt. Recd. ________
❑ CC ❑ Cash ❑ Check ❑ TC ❑ PO
Check # ________
P.O. # ________
Cust. # ________
Reg./Order # ________
OPED97

Benefits of SPIE Membership

$85 in North America
$95 outside North America
$30 Student with OER, journal
$15 Student without OER, journal

Joining SPIE as a regular member provides you with many benefits including:

- opportunity to stay informed
- peer recognition
- association, communication, and networking with colleagues
- continuing education
- participation in and contribution to technical community
- voting privileges
- eligibility to hold SPIE office
- professional growth
- exploration of emerging applications and technologies
- subscription to *OE Reports*, SPIE's monthly newspaper
- subscription to any one of SPIE's three journals
- career enhancement
- special member rates
- access to Professional Group Benefits Program

Student and Retired Memberships are available at reduced rates.

To apply, complete the membership application at left. Send the completed form to SPIE, P.O. Box 10, Bellingham, WA 98227-0010 USA. Phone: 360/676-3290; fax: 360/647-1445; e-mail: spie@spie.org; telnet FTP: spie.org; World Wide Web URL: http://www.spie.org/.

Corporate Sustaining Memberships are available to companies, corporate divisions, or associations. Please request our brochure detailing benefits.

Working Groups

SPIE working groups are global, interactive networks of professionals and organizations working in specific technologies. They are designed to help members expand their knowledge and stay abreast of current events by communicating directly with others in their field. Working groups will allow you to economically identify and contact hundreds of experts throughout the world working on similar problems, and to help SPIE and other sponsoring organizations shape future conferences and publications. Benefits include:

- annual subscription to *OE Reports* newspaper
- annual directory of members (includes mail and electronic addresses)
- regular newsletter and/or regular *OE Reports* coverage of working group news and technical information
- electronic services including listserves for specific groups
- annual working group meeting
- discounts on SPIE conferences, short courses, and publications
- discounts on related publications from other publishers as available
- notification of global activities related to the group's technical activities.

Individual Membership $30
(Full SPIE members pay $15).
Corporate Memberships are available. Contact SPIE for details.

INDEX TO ADVERTISERS

CORPORATE MEMBER ADDRESS LIST

Australian Holographics Studios Pty Ltd
PO Box 160
Kangarilla
SA 5157
Tel: (08) 383 7255
Fax: (08) 383 7244
austholo@camtech.net.au

AVIMO Electro-Optics Pty Ltd
14 Fifth Lok Yang Road
Singapore, 2262
Tel: +65 265 5122
Fax: +65 265 1479

British Aerospace Australia
PO Box 180
Salisbury SA 5108
Head Office:
14 Park Way
Technology Park
The Levels, SA 5095

Coherent Scientific Pty Ltd
116 Burbridge Road
HILTON, SA, 5033
Tel: (08) 8352 1111
Fax: (08) 8352 2020
cohsci@cohsci.com.au

Electro Optic Systems
55A Monaro St
Queenbeyan, NSW, 2620
Tel: (06) 299 2470
Fax: (06) 299 2477

Electro Optics Pty Ltd
PO Box 67
Kenthurst, NSW, 2156
Tel: (02) 9654 1873
Fax: (02) 9654 1539

Francis Lord Optics
33 Higginbotham Rd
Gladesviile, NSW, 2111
Tel: (02) 9807 1444
Fax: (02) 9809 7136

Hadland Photonics Pty Ltd
19A Hampsbire Road
Glen Waverley, VIC, 3150
Tel: (03) 9560 2366
Fax: (03) 9560 8402

Jung Precision Optics
Bld 186
Contractors Area
Salisbury, SA, 5108
Tel: (08) 8287 2422
Fax: (08) 8287 2706

Kidger Optics Limited
9a High Street
Crowborougb, East Sussex
TN6 2QA
UK
Tel: +44 1892 663555
Fax: +44 1892 664483
sales@kidger.demon.co.uk

Laser Electronics (operations) Pty Ltd
PO Box 359
Southport
QLD, 4215
Tel: (075) 96 0177
Fax: (075) 96 3530

Lastek Pty Ltd
GPO Box 2212
Adelaide, SA, 5001
Tel: (08) 8443 8668
Fax: (08) 8443 8427
lastek@saschools.edu.au

OptiScan Pty Ltd
PO Box 1066
Mt. Waverley MDC
VIC 3149
Tel: (613) 9562 7741
Fax: (613) 9562 7742

Photon Engineering
PO Box 10269, Gouger St
Adelaide SA 5000
Tel: (08) 8410 4599
Fax: (08) 8410 4544
photeng@ozemail.com.au

Raymax Applications Pty Ltd
16 Ross Street
Newport Beach, NSW, 2106
Tel: (02) 9979 7646
Fax: (02) 9979 8207

Rofin Australia Pty Ltd
Unit 4 42-44 Garden Boulevard
Dingley, VIC, 3172
Tel: (03) 9558 0344
Fax: (03) 9558 0252

Spectra-Physics Pty Ltd
25 Research Drive
Croyden, VIC, 3136
Tel: (03) 9761 5200
Fax: (03) 9761 5600

Warsash Scientific Pty Ltd
PO Box 1685
Strawberry Hills, NSW, 2012
Tel: (02) 9319 0122
Fax: (02) 9318 2192
warsash@ozemail.com.au

AUSTRALIAN OPTICAL SOCIETY

1997

Subscription Renewal Form

Please complete all details:

Postal Address

Title

Initials

First Name(s)

Surname

Employer/Institute/Company

Telephone Number

Fax Number

Email

Affliliations AIP OSA SPIE

Main Activities (number up to three in order of importance)

First Second Third

1	astronomical optics	8	optical design	15	nonlinear optics
2	atmospheric optics	9	optical physics	16	teaching
3	communications and fibres	10	radiometry, photometry & colour	17	holography
4	electro-optics	11	spectroscopy	18	(......................................)
5	fabrication and testing	12	thin films	19	(......................................)
6	information processing	13	vision	20	(......................................)
7	lasers	14	quantum optics		

SUBSCRIPTION RATES (per calendar year)

Corporate : A$ 250 p.a. Associate: A$ 125 p.a. Member: A$30 p.a. Student: A$10 p.a.

PAYMENT METHOD *(Please tick box)*

*Cheque** O *Mastercard* O

Money order O *Bankcard* O

Visa O

Send payments to:

A/Prof Barry Sanders, HonTreasurer AOS
School of MPCE, Macquarie University
Sydney, NSW 2109
Tel: 02 9850 8935 Fax: 02 9850 8115
email: barry@mpce.mq.edu.au

* Cheques payable to "THE AUSTRALIAN OPTICAL SOCIETY"

If paying by credit card please <u>complete</u> ALL boxes in this authorization. Incomplete forms cannot be processed.

EXPIRY DATE /

CARD NUMBER

CARDHOLDER AMOUNT A$

SIGNATURE DATE

* Please do not staple cheques onto this form, use a paperclip instead.